

Supplemental Materials

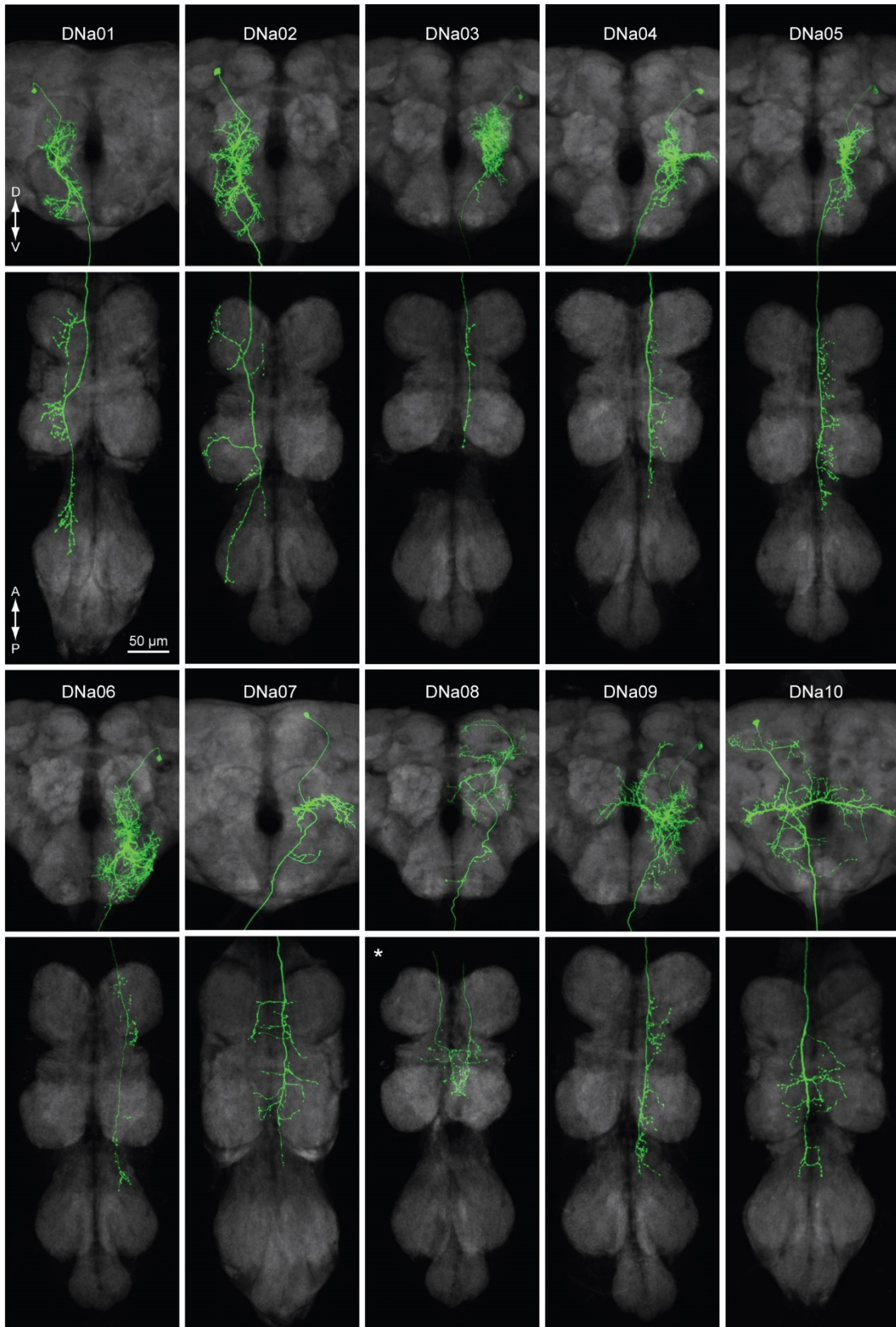
The functional organization of descending sensory-motor pathways in *Drosophila*

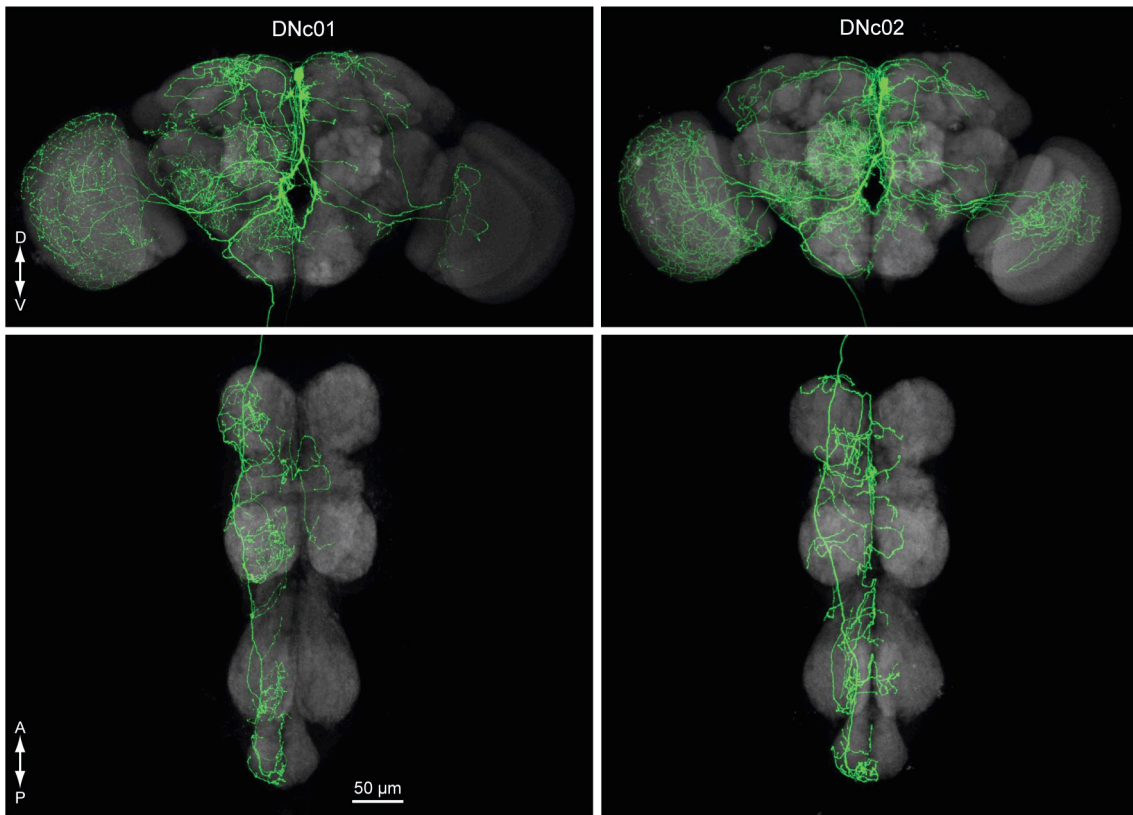
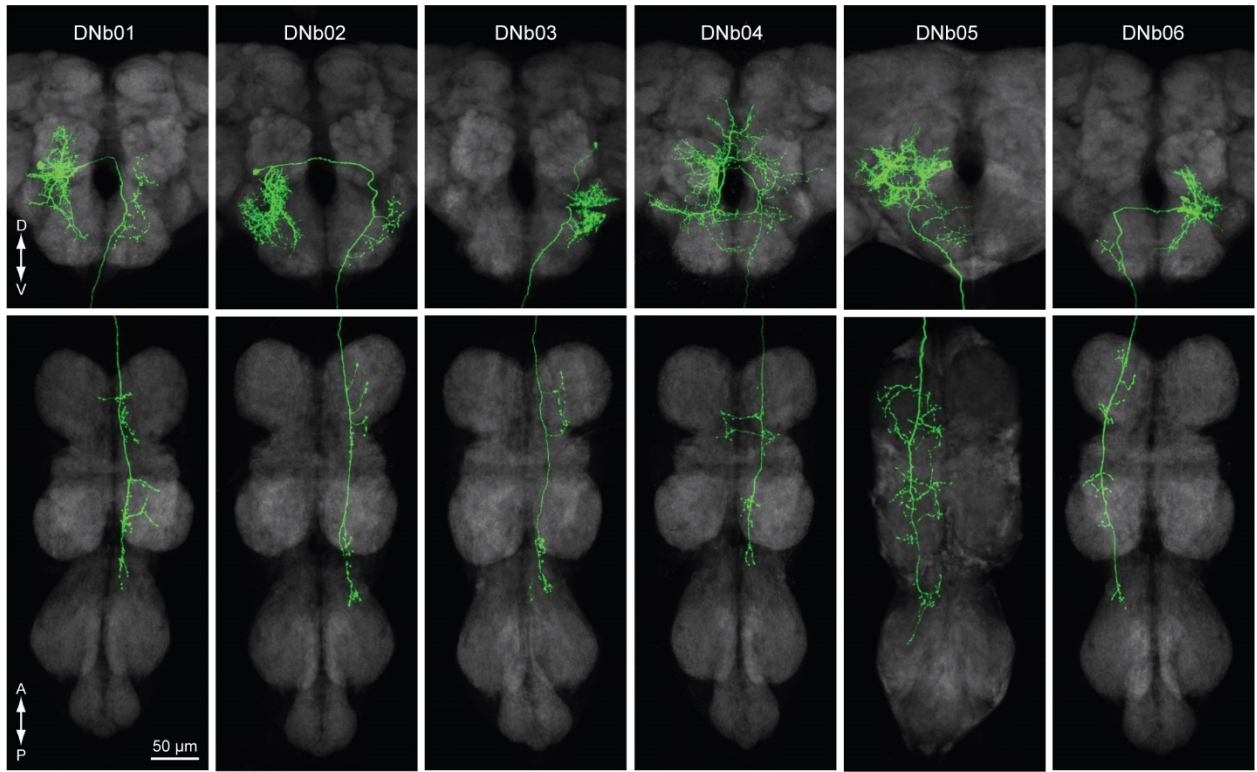
Shigehiro Namiki,¹ Michael H. Dickinson,² Allan M. Wong,¹ Wyatt Korff,¹ Gwyneth M. Card,^{1,*}

¹*Janelia Research Campus, Howard Hughes Medical Institute, Ashburn, VA 20147, USA*

²*Division of Biology and Bioengineering, California Institute of Technology, Pasadena, CA 91125, USA*

*Correspondence should be addressed to cardg@janelia.hhmi.org (G.M.C)





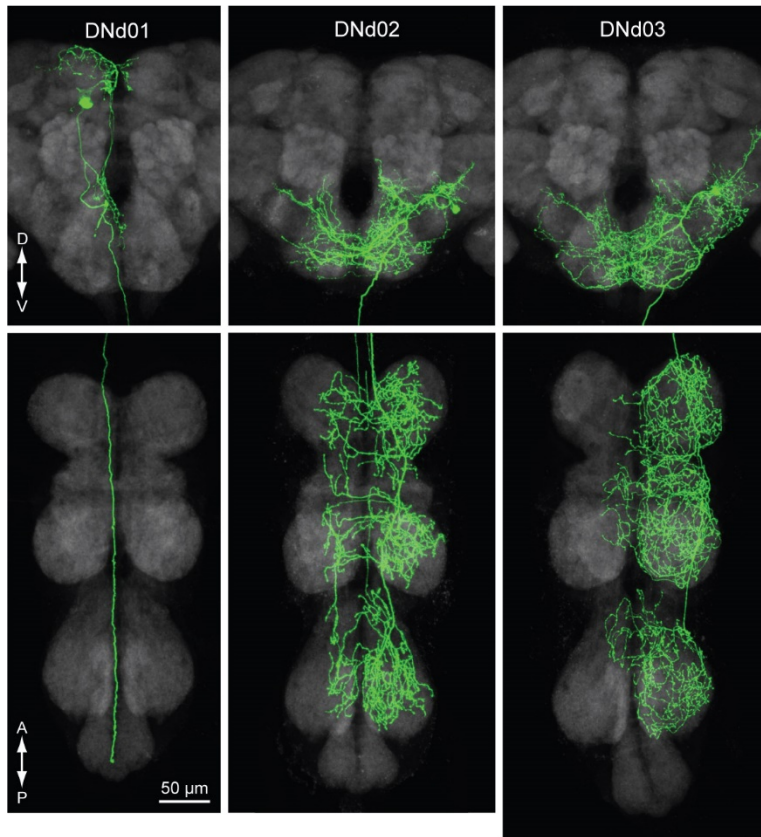
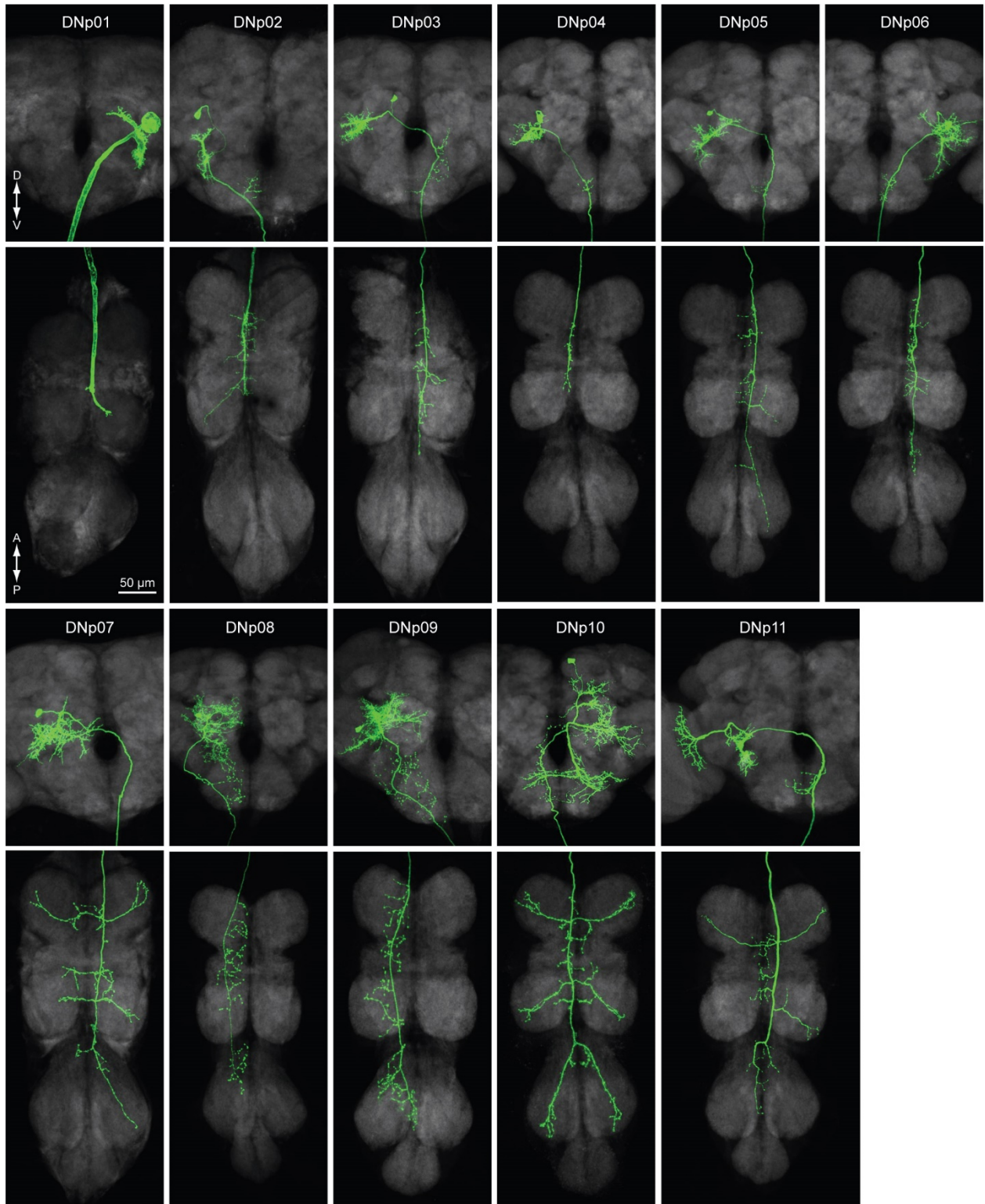
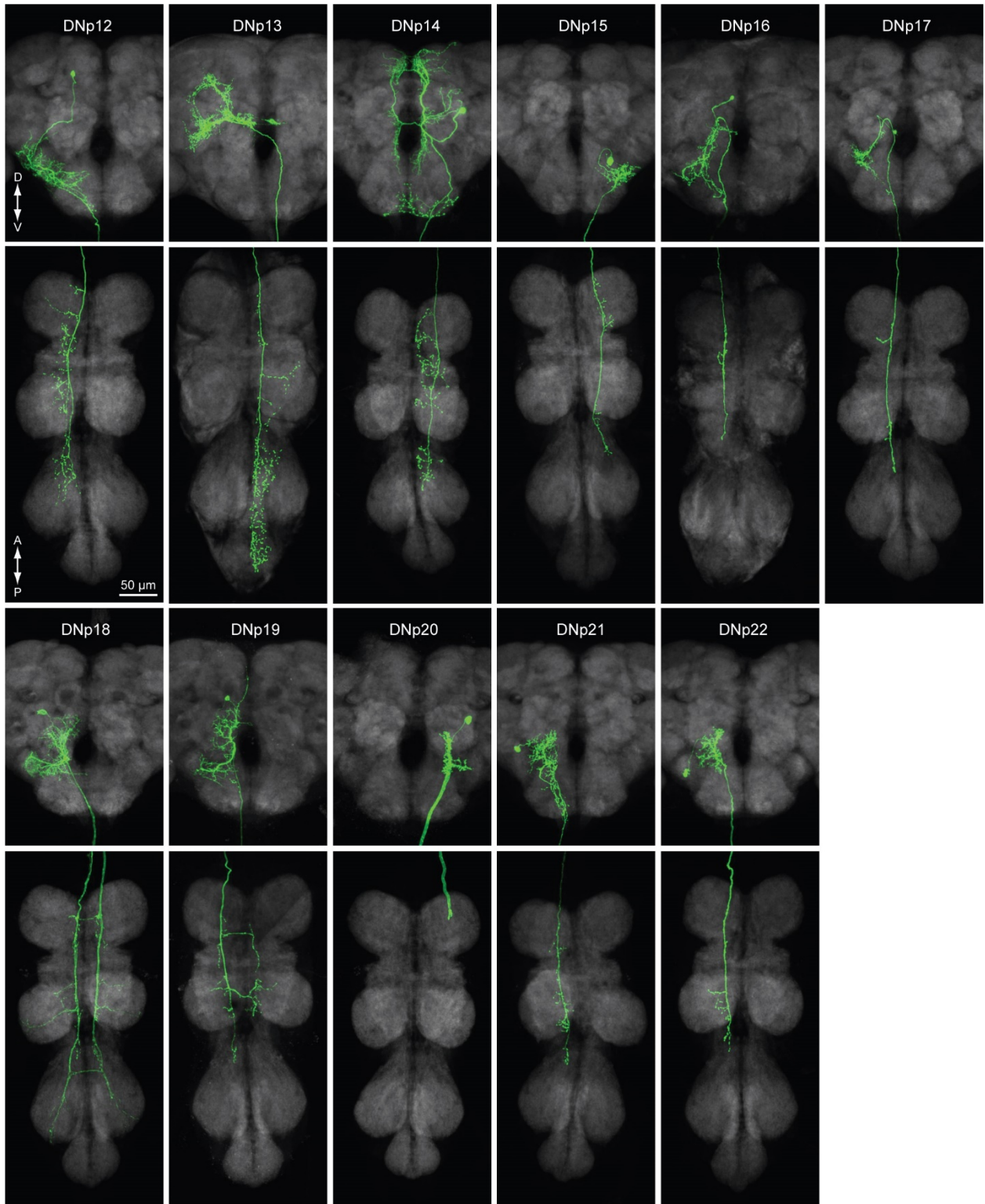
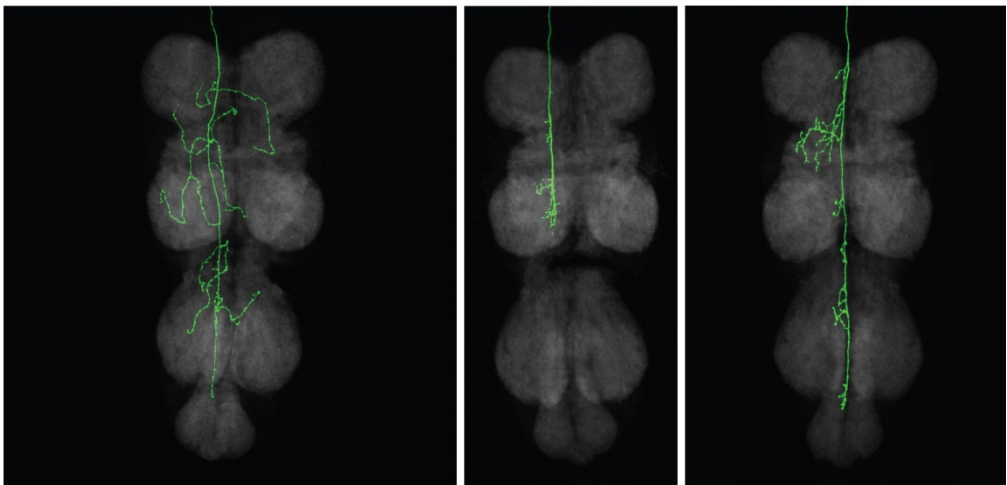
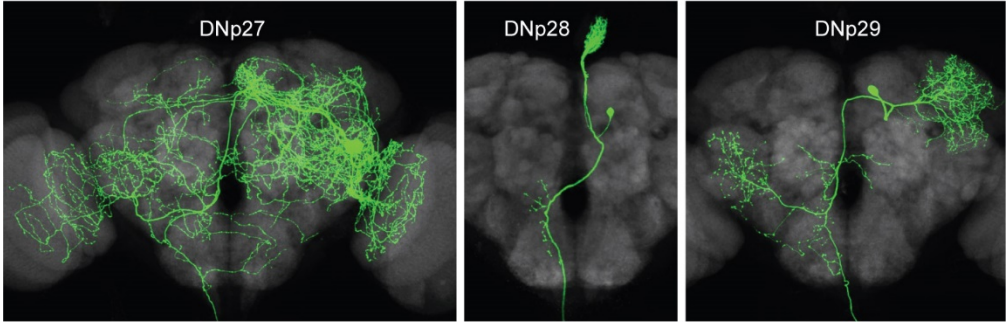
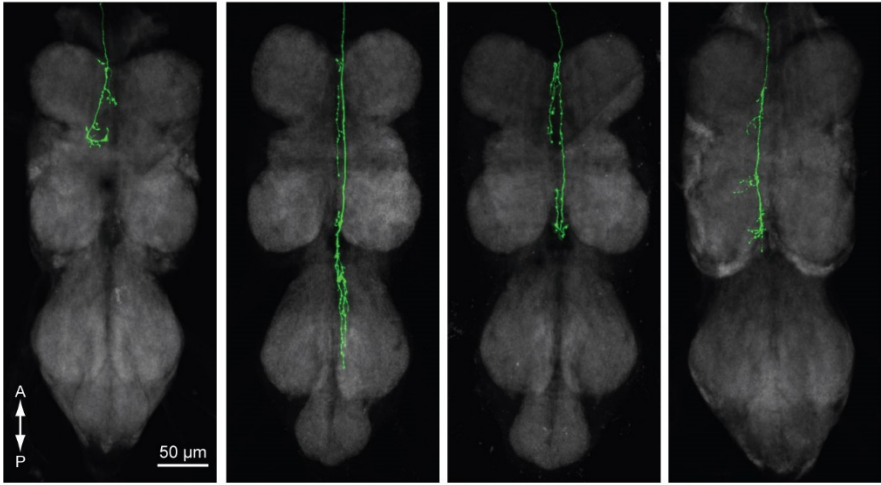
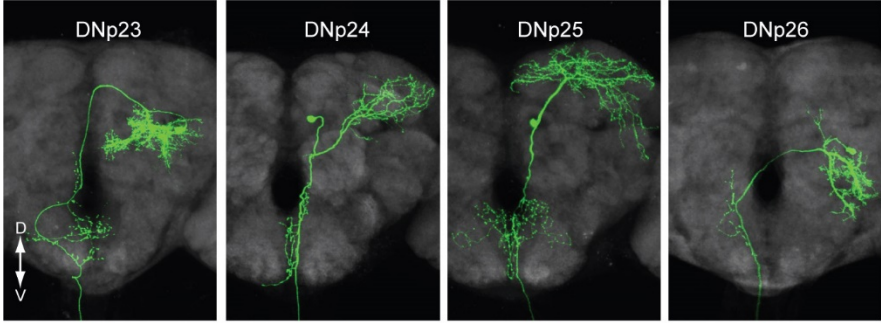


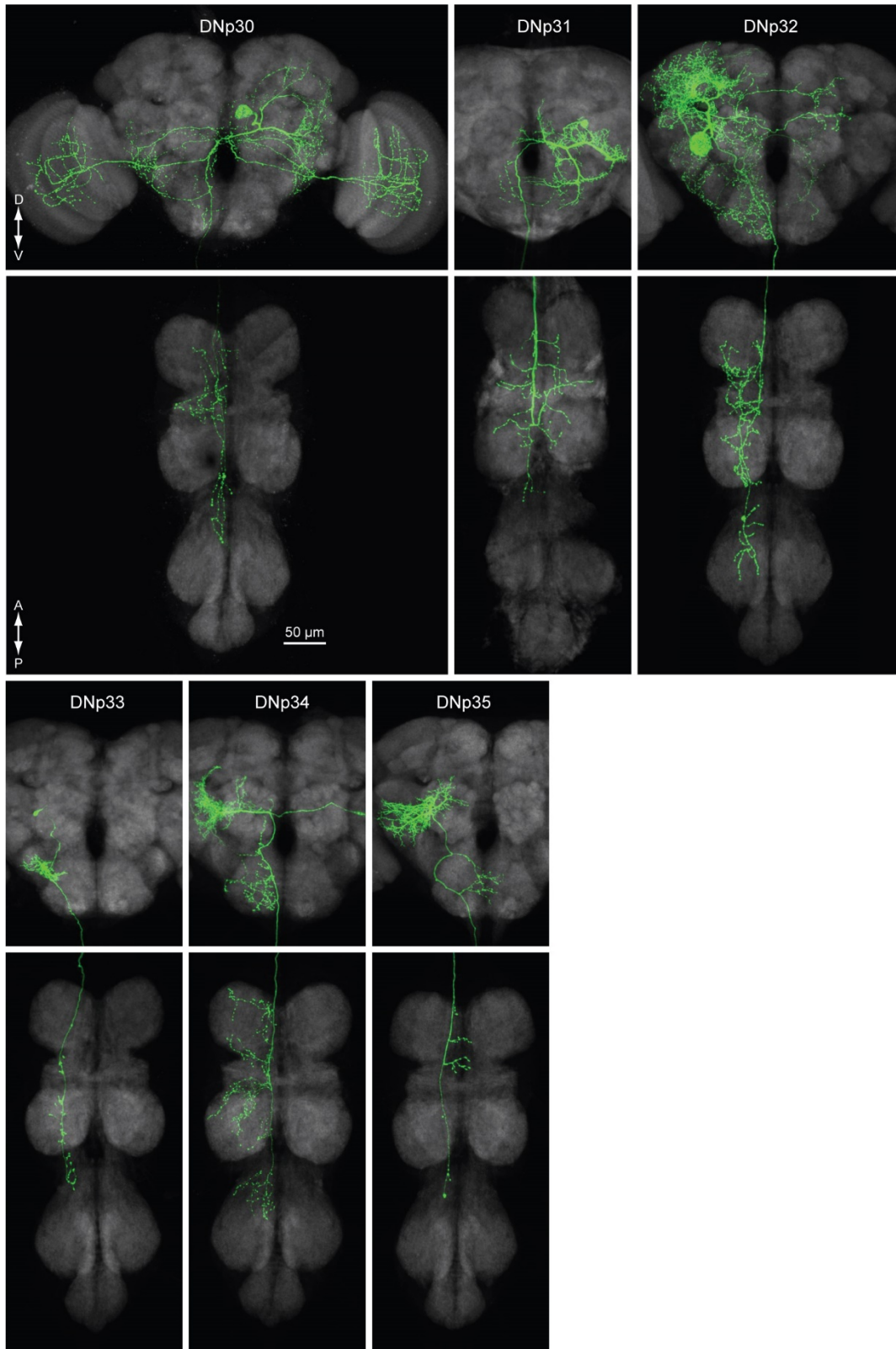
Figure 2. Figure supplement 1. Morphology of DNs (1/4).

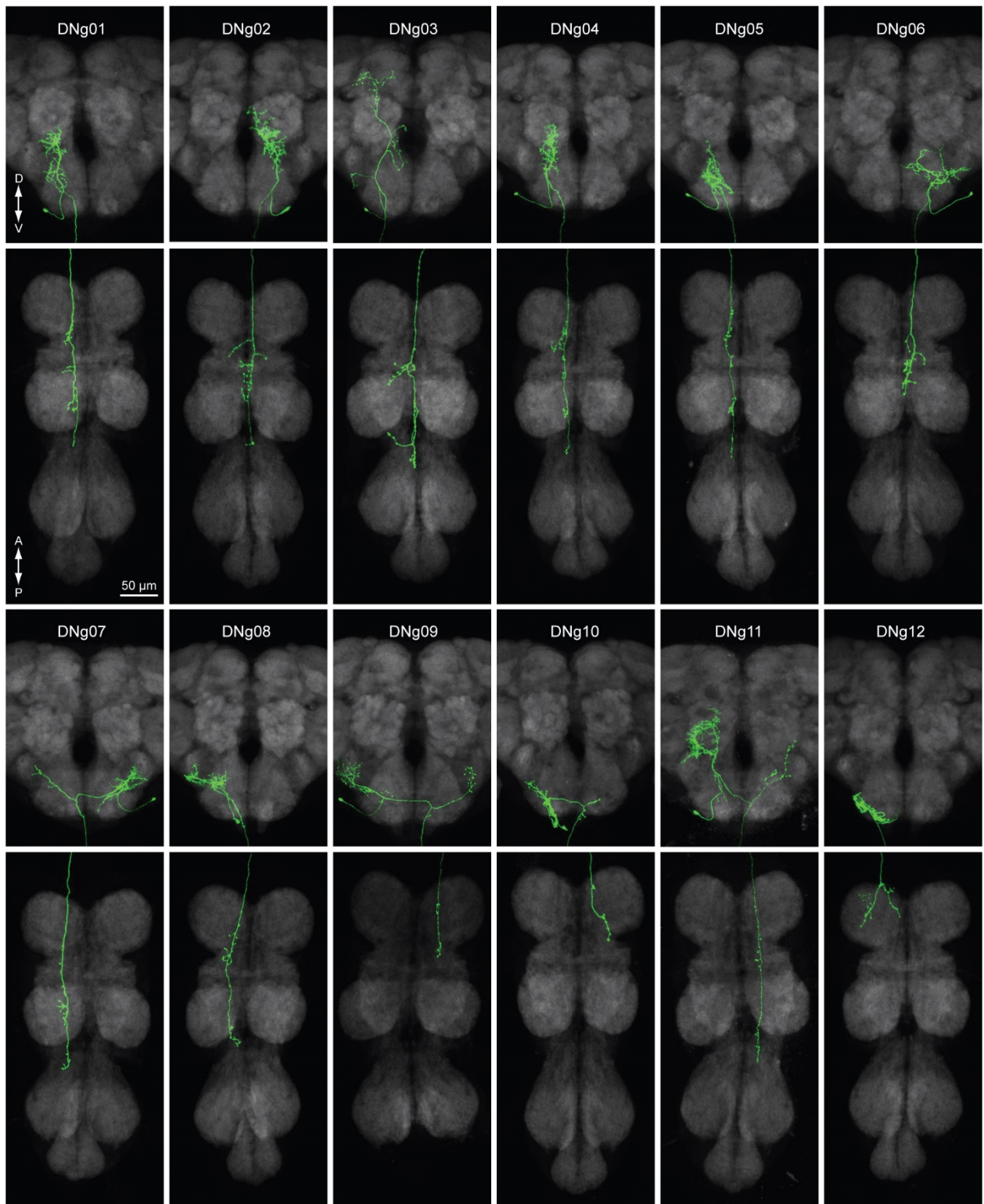
Morphology of identified DNs, groups a-d. Images are masks for single DNs made from maximum intensity projections of confocal images for sparse split lines. Shown here as horizontal views of the brain (*top*) and VNC (*bottom*).

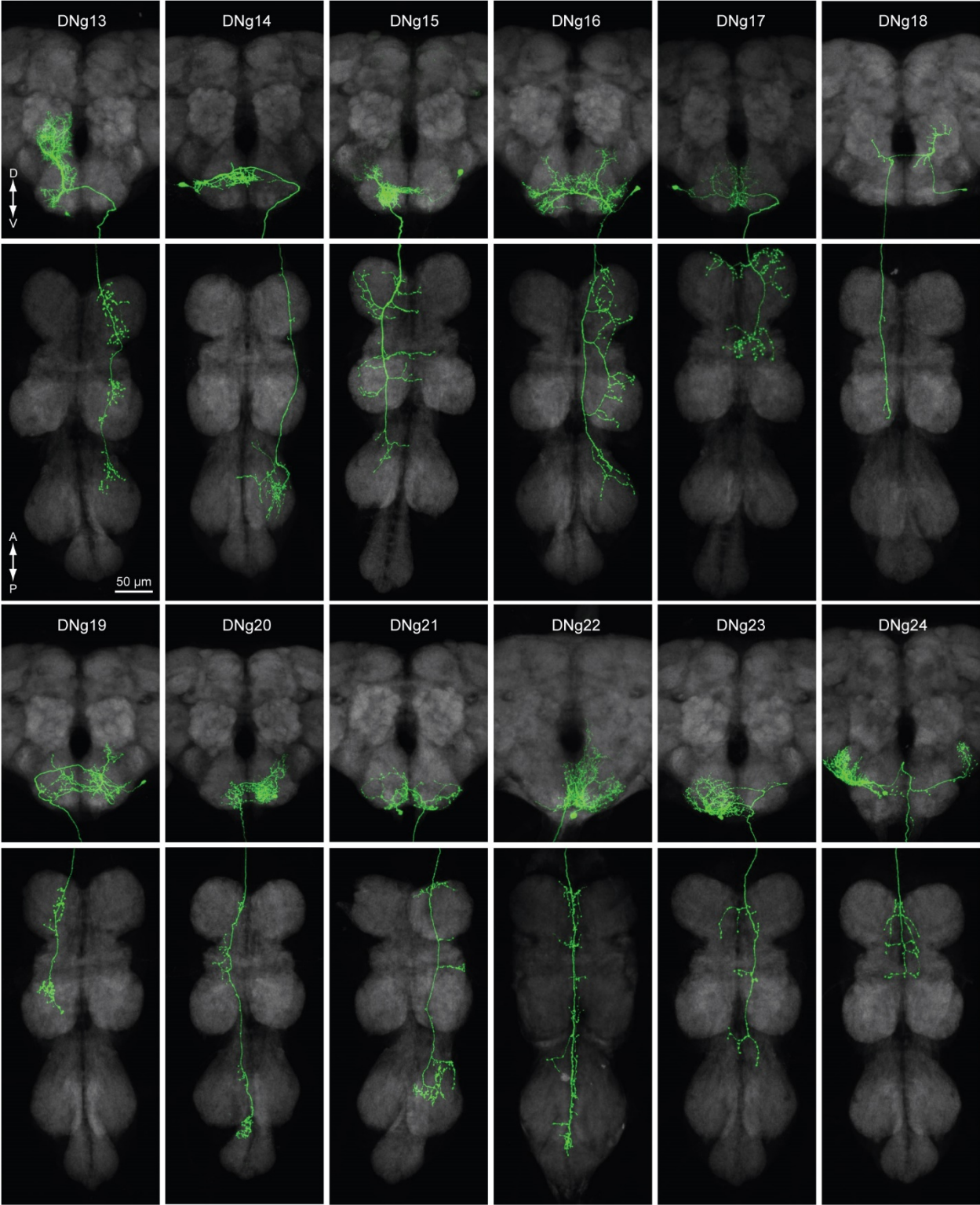


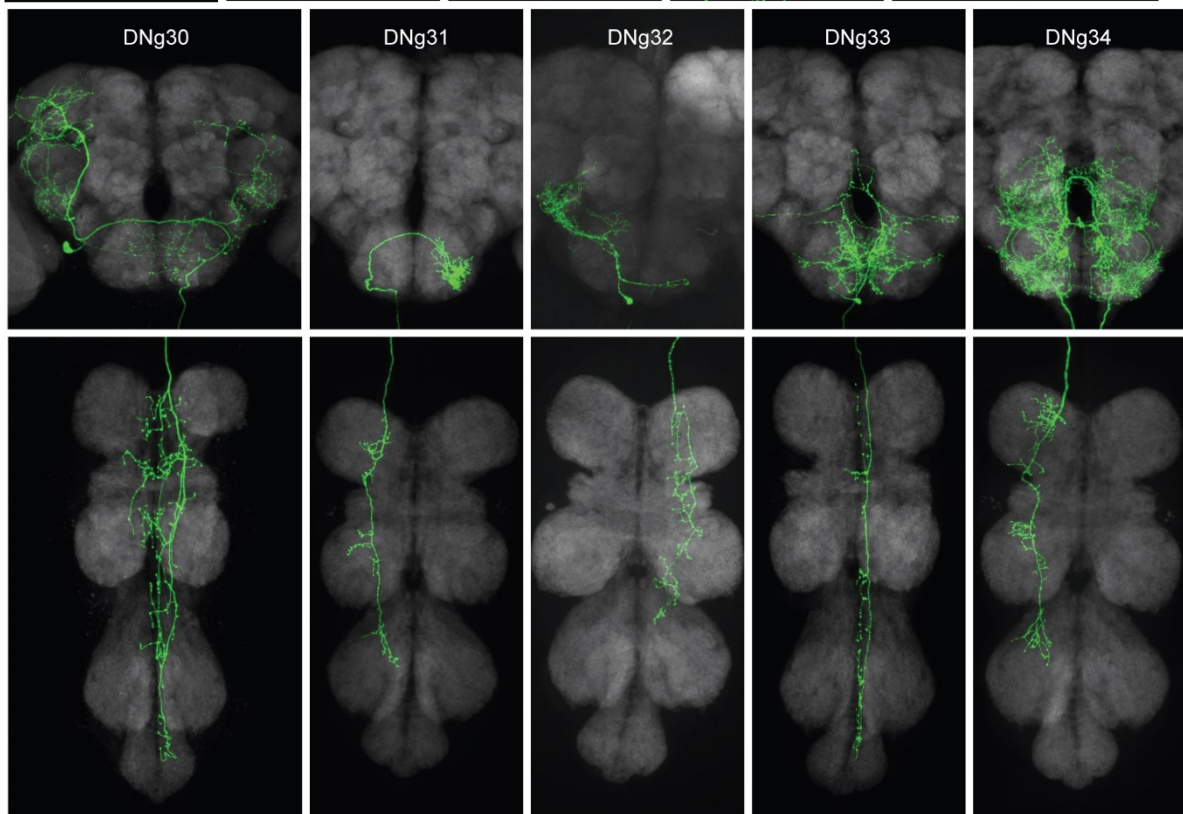
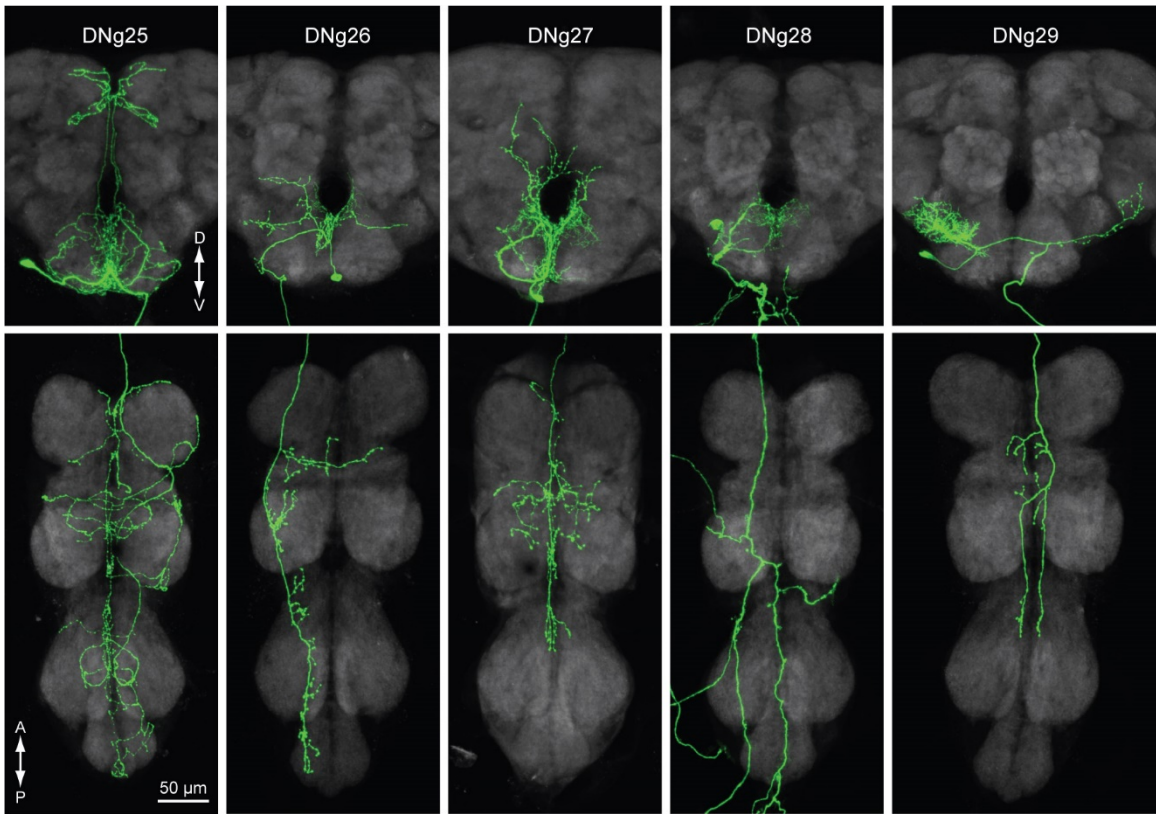












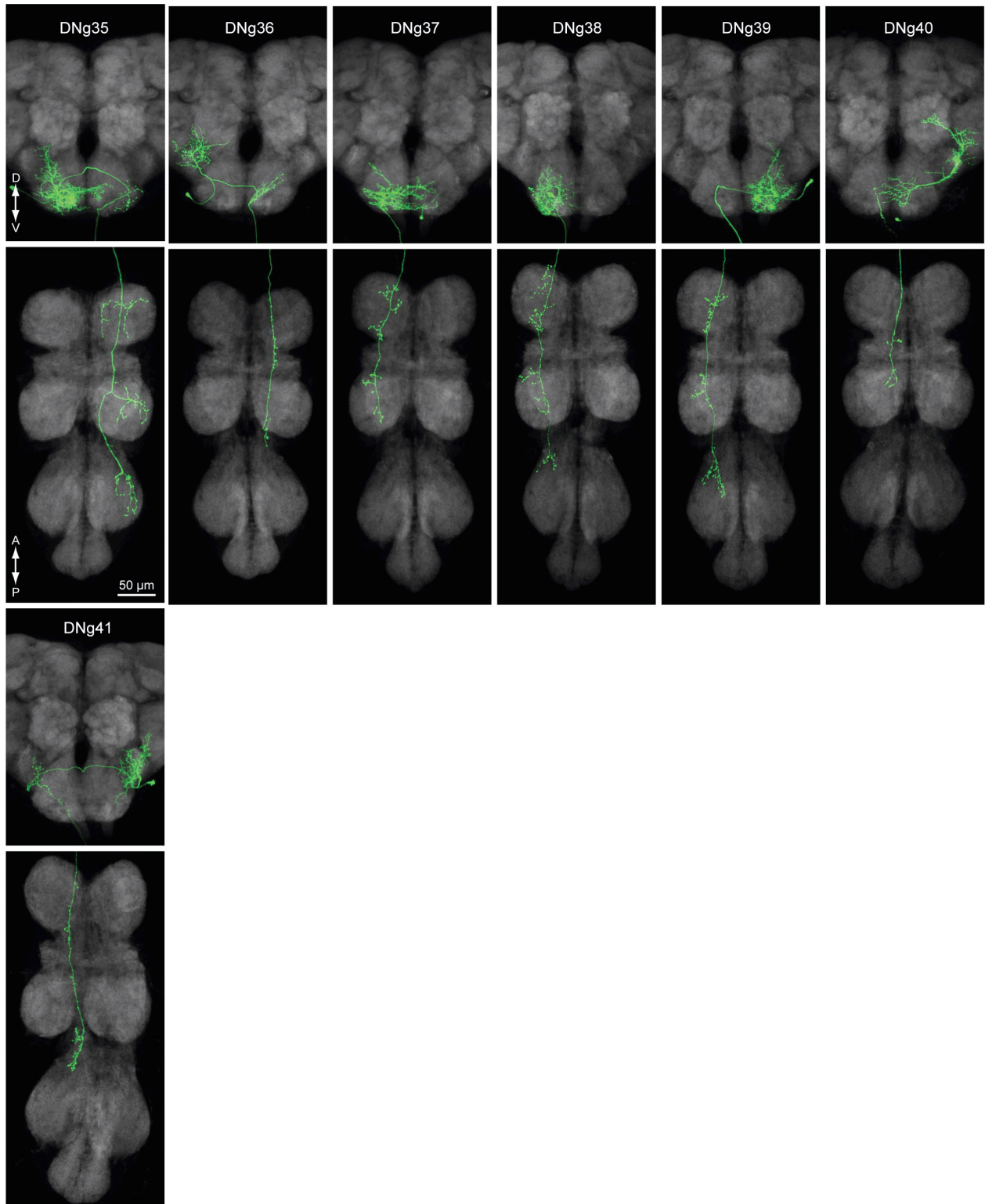


Figure 2. figure supplement 3. Morphology of DNs (3/4).

Morphology of identified DNs, group g, whose somata are located on the gnathal ganglion.

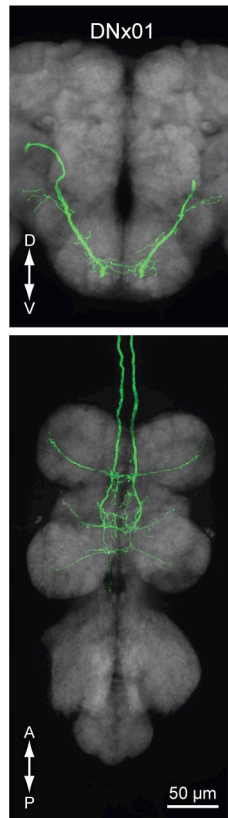


Figure 2. figure supplement 4. Morphology of DNx (4/4).

Morphology of identified DN, group x, whose soma is located outside the brain.

Figure 3—figure supplement 1

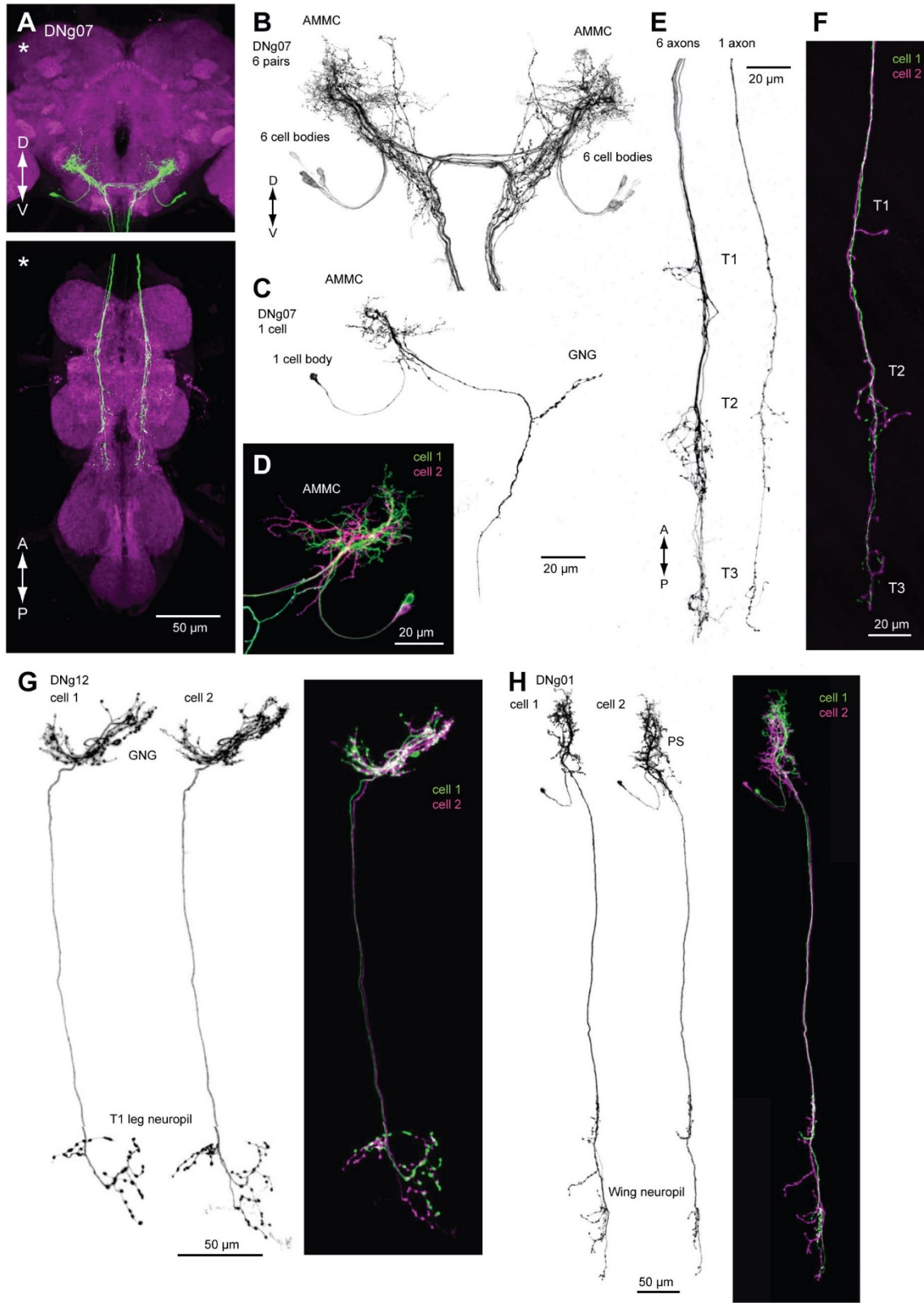


Figure 3. figure supplement 1.

(A) An example of the morphology of DN_g07 population.

(B) Confocal image of brain innervation for the sample with 6 pairs of DN_g07 type neurons.

(C) Confocal image of brain innervation for the sample with a single DN_g07.

(D) Multicolor flip-out of the DN_g07 population shows two different neurons in that type.

(E-F) The corresponding VNC projection images for samples with 6 or a single DN, as in B-D.

(G-H) Morphology of individual neurons in population DN types (G) DN_g12 and (H) DN_g01. Individual morphologies and merged image are shown.

Figure 4—figure supplement 1

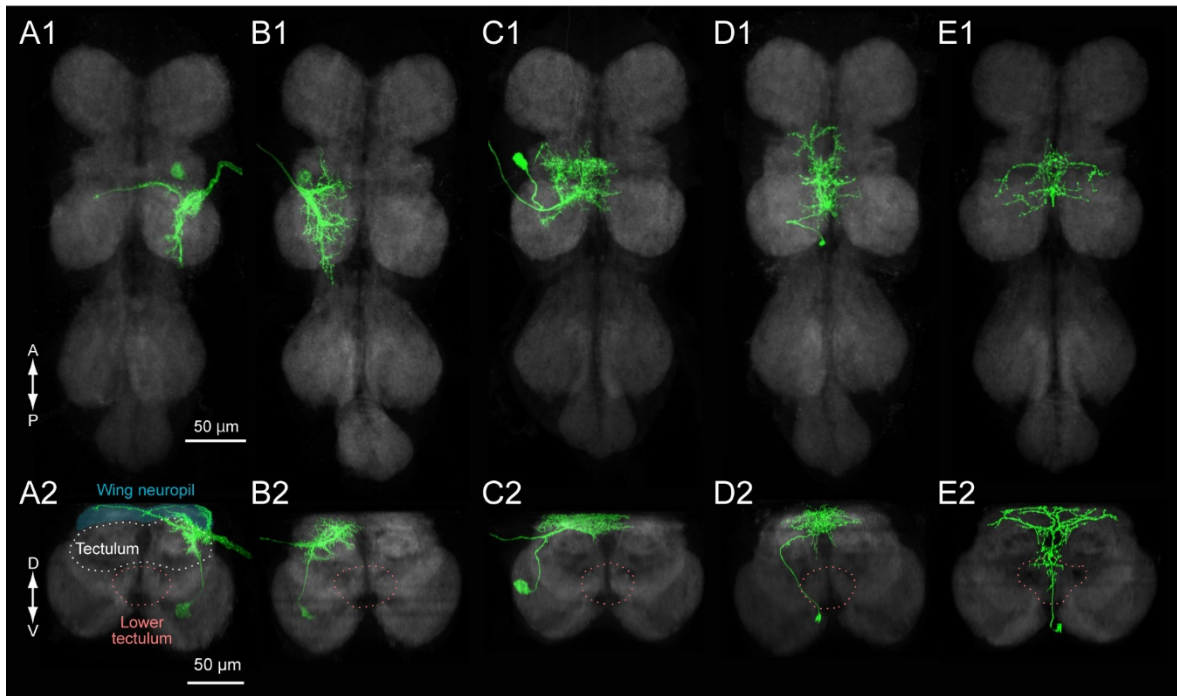


Figure 4. figure supplement 1. Morphology of interneurons innervating the wing neuropil.

(A-E) Isolated morphologies of wing muscle motor neurons for (A) steering muscle b1 (mn**b**1), (B) steering muscle b2 (putative), (C) a dorsoventral power muscle (DVM), as well as two wing neuropil local interneurons (D, E). The horizontal view of whole VNC (*top*) and the frontal view of T2 segment are shown (*bottom*). The area of the wing neuropil is shaded with light blue in A2. The areas of tectulum and lower tectulum are indicated with white (A2) and red (B2-E2) dotted lines, respectively. These example moto- and interneurons from the wing neuropil rarely innervate the lower tectulum.

Figure 4—figure supplement 2

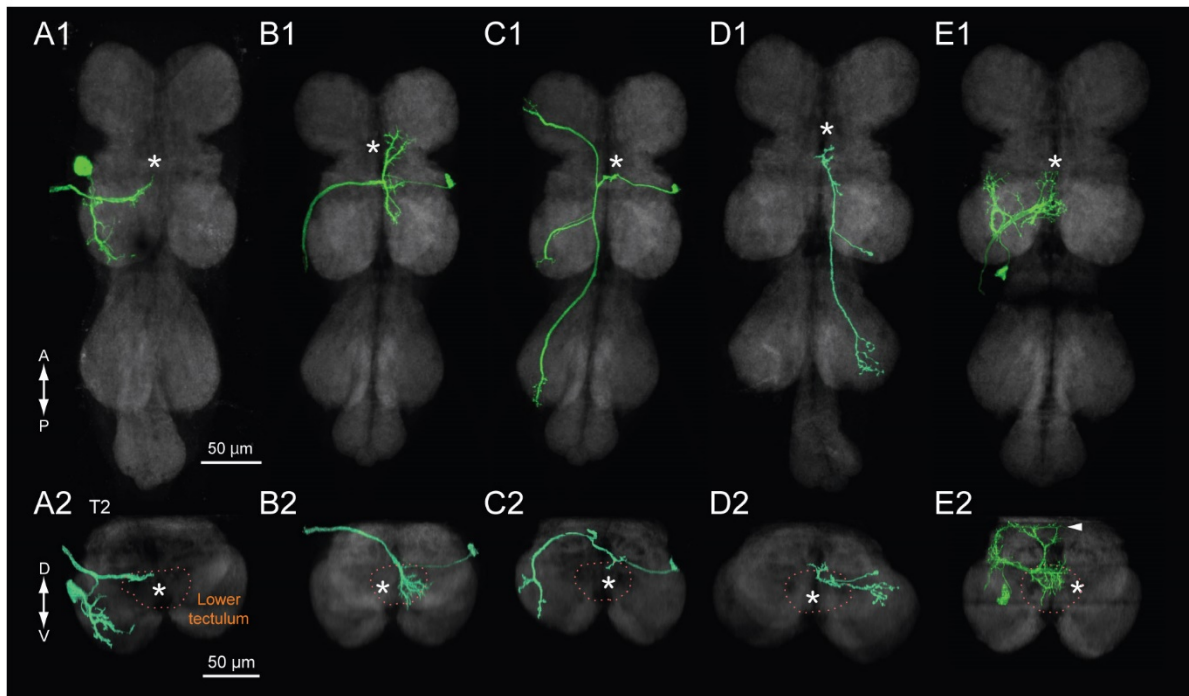


Figure 4. figure supplement 2. Morphology of interneurons innervating the lower tectulum.

(A-E) Isolated morphologies for motorneurons and interneurons innervating the lower tectulum, including two neurons postsynaptic to the giant fiber (the tergotrochanteral muscle motor neuron, TTMn (A) and the peripheral synapsing interneuron, PSI (B)), two intersegmental interneurons (C-D), and unknown motorneurons (E). Images as in Figure 4—figure supplement 1. The gross position of the lower tectulum is shown with an asterisk and orange dotted line. The smooth processes (inputs) of A-D are confined within the lower tectulum; E has smooth processes in wing neuropil and lower tectulum.

Figure 5—figure supplement 1

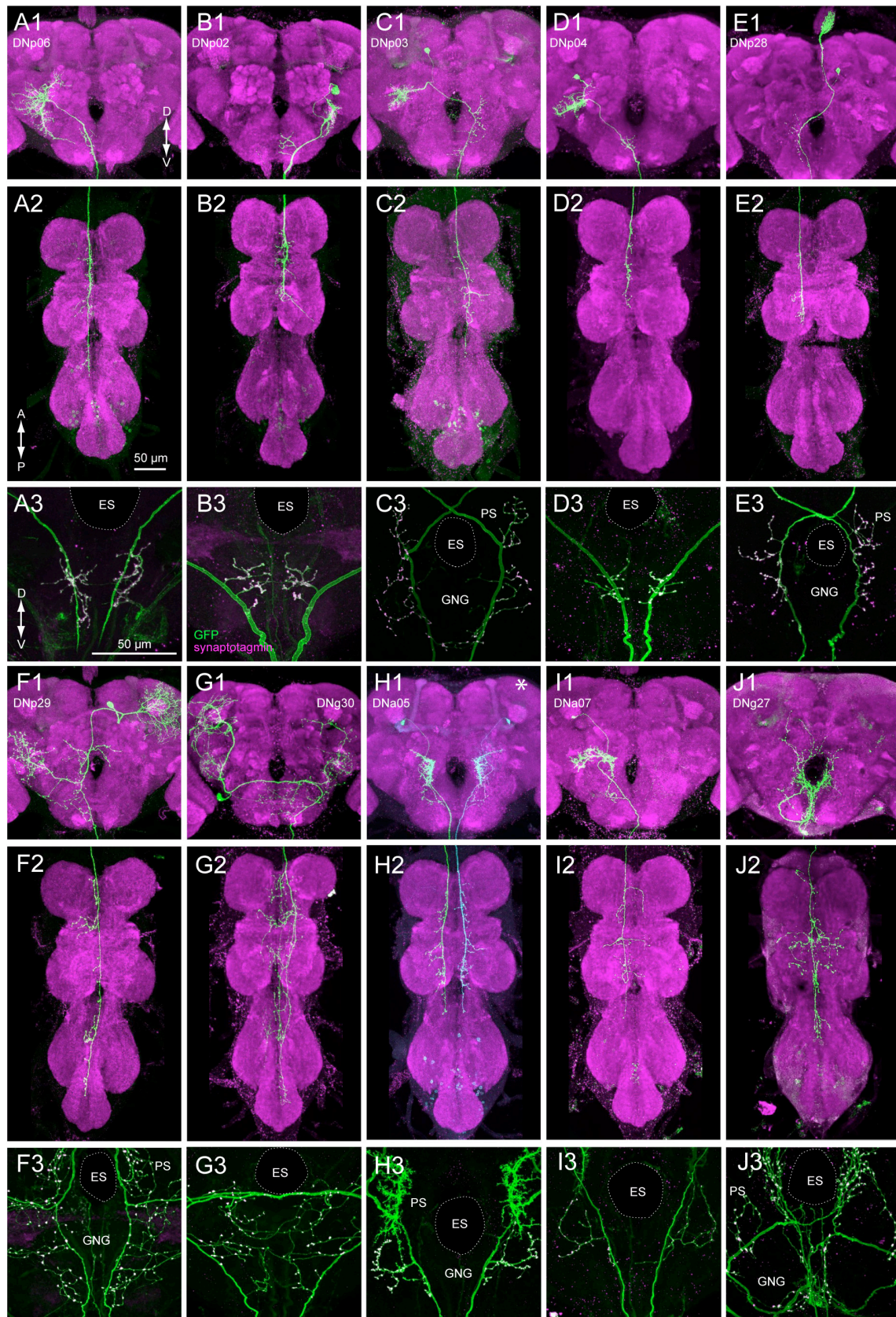


Figure 5. figure supplement 1. DN presynaptic terminals in the gnathal ganglion.

DN innervation in the brain (A1-J1) and VNC (A2-J2) obtained with the multicolor flip-out technique, and the corresponding result of synaptotagmin labeling in the GNG (A3-J3). Ten examples of DNs with varicose process in the GNG are shown.

Figure 5—figure supplement 2

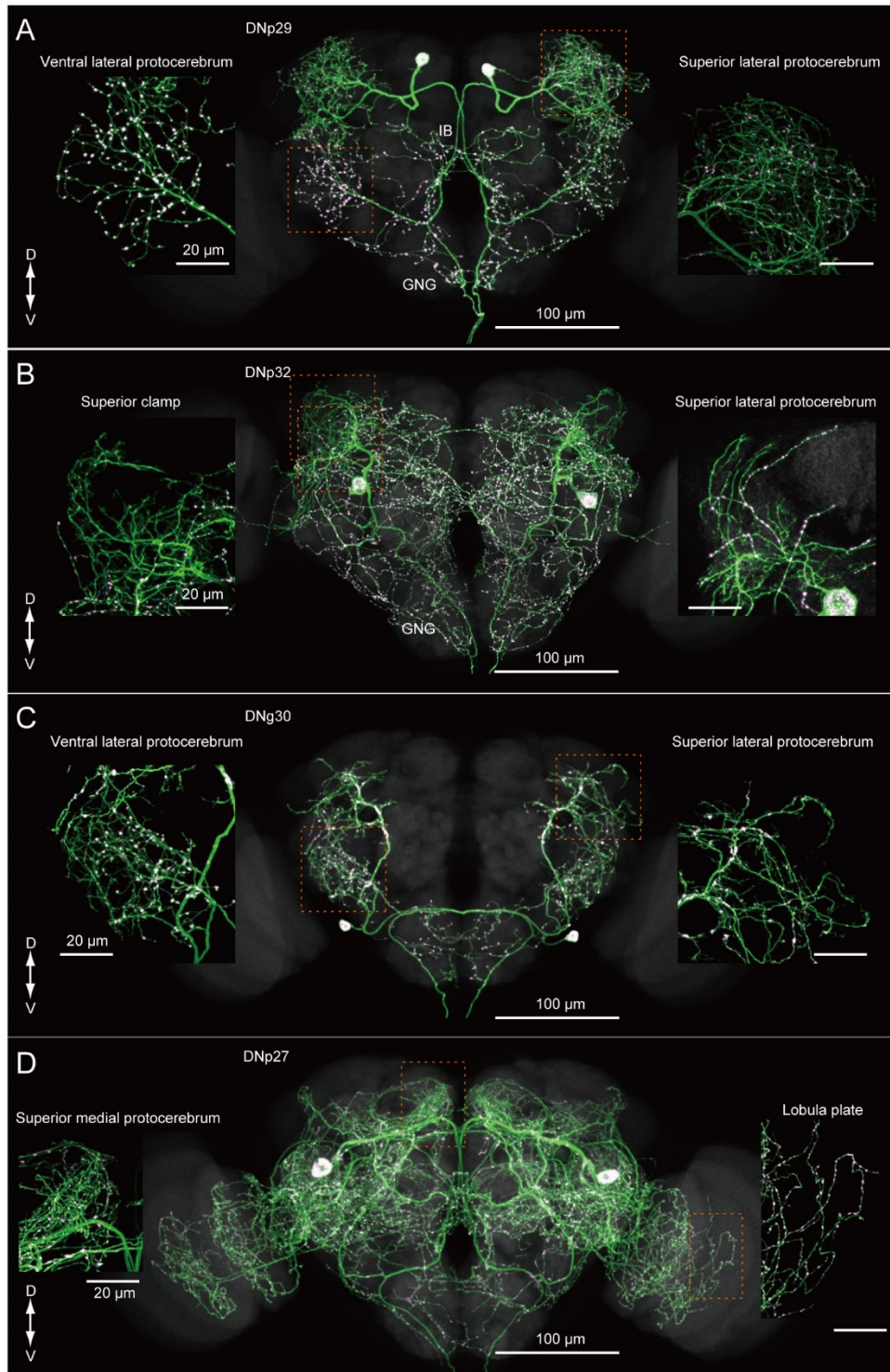


Figure 5. figure supplement 2. DN presynaptic terminals in the brain.

The result of synaptotagmin labeling of split-GAL4 lines targeting four DN types with prominent varicose endings in the brain. Insets show magnification of regions indicated by orange dotted lines.

(A) Morphology of DNp29. A neuron with similar morphology has been described in *Drosophila* (SP1; Nässel, 1993, Figure 4). The DN has both smooth and varicose processes in the superior lateral protocerebrum. Varicose processes are dominant in other regions.

(B) Morphology of DNp32. A neuron with similar morphology in the brain has been described in *Drosophila* (DN1, Tanaka et al., 2012, Figure 8). The DN has smooth process in the superior and inferior clamp, superior lateral protocerebrum and posterior lateral protocerebrum. Varicose processes are dominant in other regions.

(C) Morphology of DNg30. Both smooth and varicose process are observed in the superior lateral protocerebrum and anterior ventral lateral protocerebrum. Varicose processes are dominant in other regions. The morphologies in the brain and VNC are similar to those of the natalisin-positive neurons, called inferior contralateral interneurons (Jiang et al., 2013, Figure 2)

(D) Morphology of DNp27. Smooth processes are only observed in the superior medial protocerebrum. The morphology is partially similar to a known DN (GAMDN, Mu et al., 2014), but DNp27 lacks the innervation to the antennal mechanosensory motor center.

Figure 5—figure supplement 3

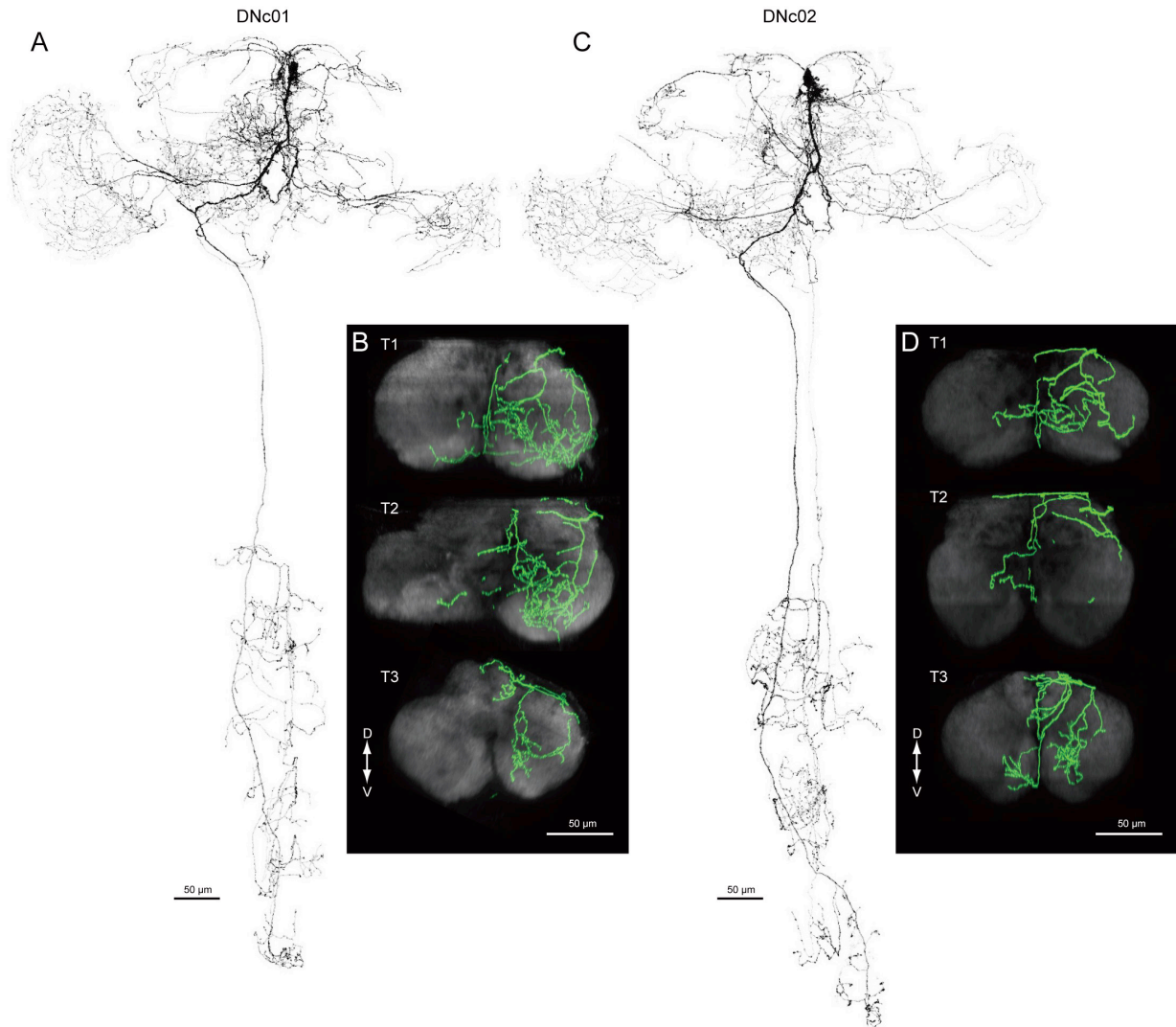


Figure 5. figure supplement 3. DNs in the pars intercerebralis.

(A-D) Morphology of DNc01 and c02. Whole morphology (A, C) and horizontal views of VNC (B, D) are shown. Both cell types have their cell body located in the pars intercerebralis, where Hsu and Bhandawat (2016) also observed DNs. c01, but not c02, has a varicose process in the mushroom body lobe, and both have varicose processes in the fan-shaped body, protocerebral bridge, and the mushroom body calyx. c02, but not c01, has a varicose process in the lobula. Both c01 and c02 project to leg neuropils as well as dorsal neuropils and the medial ventral association center. However, c02 projects to the dorsal part of the leg neuropils, where c01 has no innervation.

Figure 5—figure supplement 4

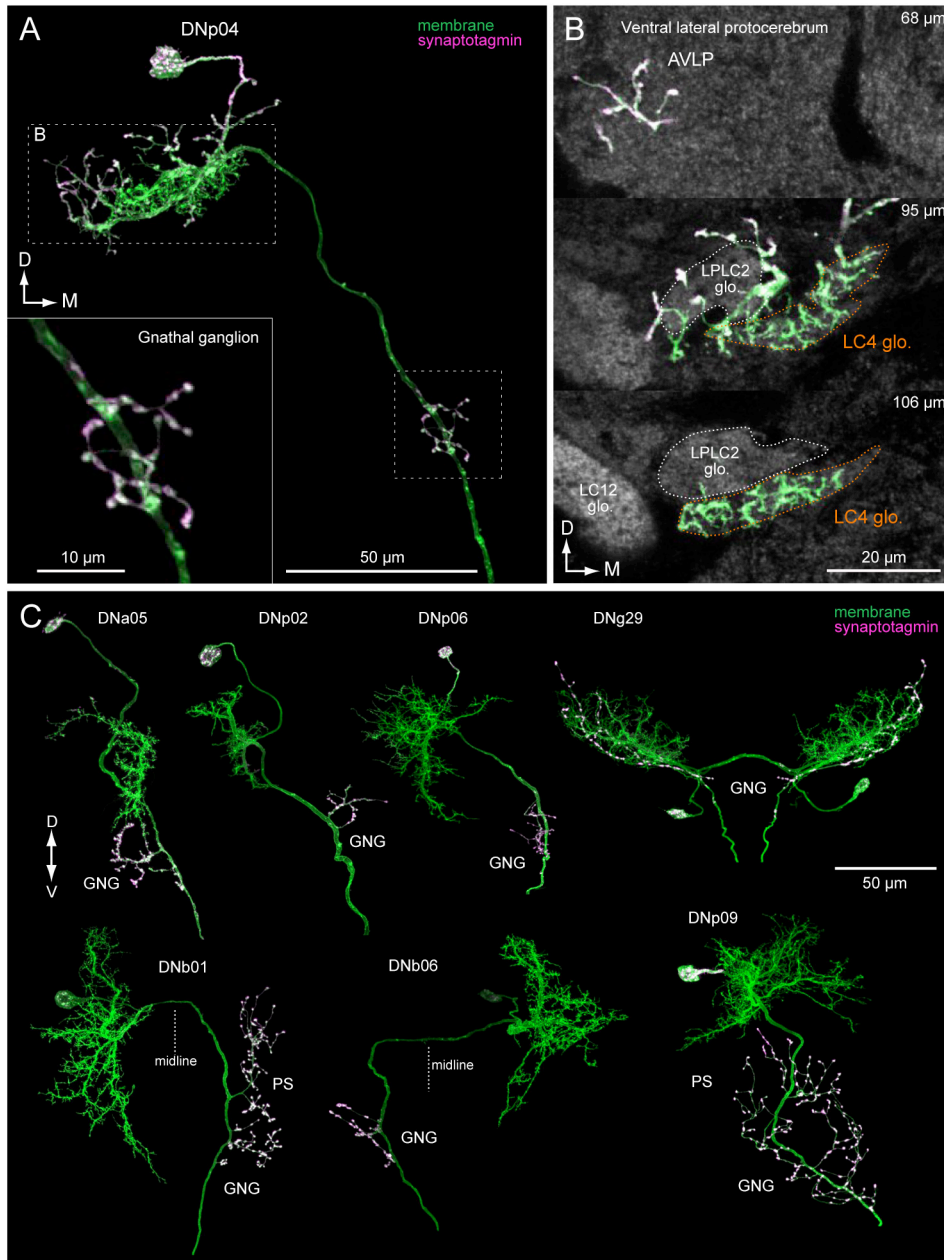


Figure 5. figure supplement 4. DN presynaptic terminals in the brain.

(A) Synaptotagmin labeling of DNp04 (green, membrane-bound GFP; magenta, synaptotagmin), shown as a maximum intensity projection of the whole morphology in the brain. Inset shows magnification of innervation in the GNG. (B) Innervation of p04 in the ventral lateral protocerebrum near the optic glomeruli. Three consecutive confocal stacks are shown with depth from the anterior brain surface indicated in *top-right*. p04 innervates the LC4 glomerulus with smooth processes and has presynaptic branches outside the glomerulus (C) Examples of synaptotagmin labeling in the brain for DNa05, p02, p05, g29 (both DNs in pair shown), b01, b06, and p09.

Figure 6—figure supplement 1

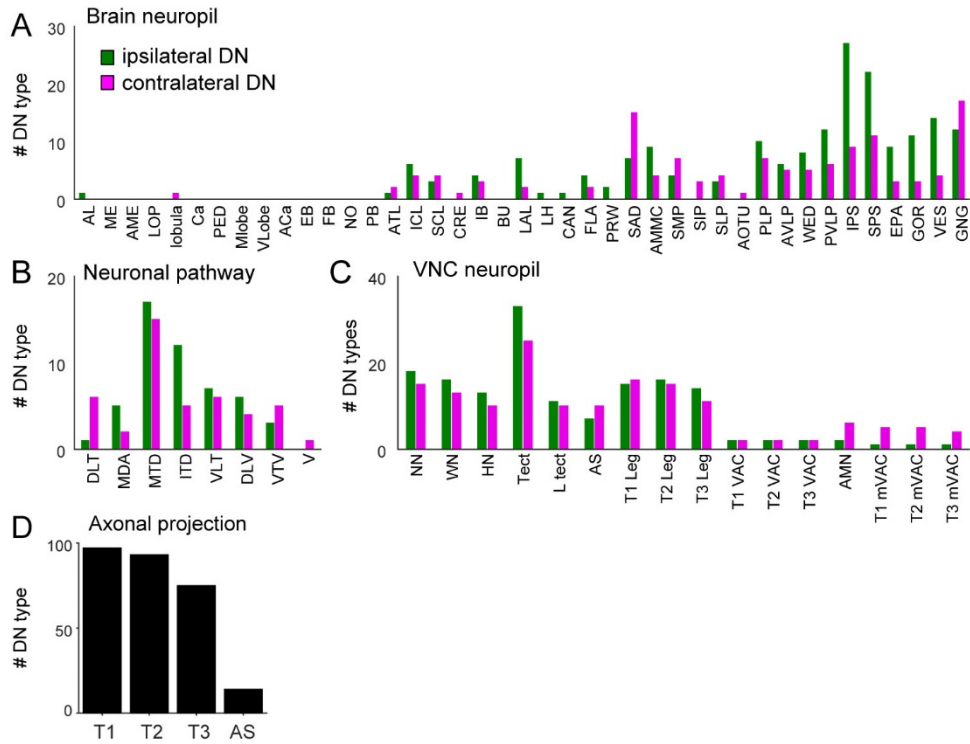


Figure 6. figure supplement 1. Laterality and extent of DN axonal projections.

(A-C) The number of DN types innervating individual brain regions (A), tracts (B), and VNC regions (C) divided into ipsilateral- (green) and contralateral- (magenta) projecting DN.

(D) The number of DN types innervating each of the four different VNC segments. The majority of DN terminated in the T3 segment. DN reaching the abdominal segment (AS) were rare.

Figure 7—figure supplement 1

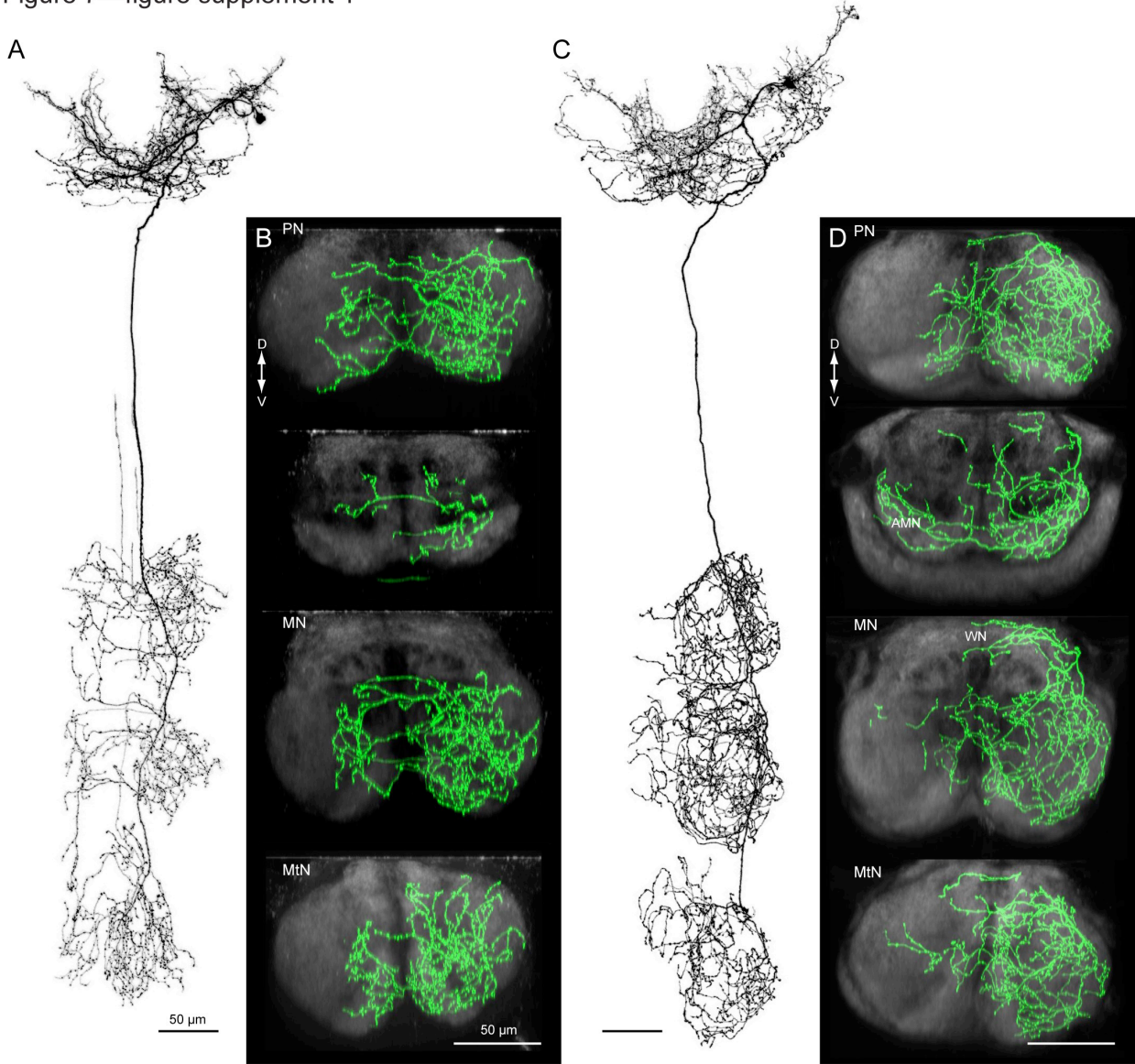


Figure 7. figure supplement 1. Putative octopaminergic DNs.

(A-B) Morphology of DNd02. Whole cell morphology (A) and frontal sections of VNC are shown (B).

The cell body is located in the GNG and the axon descends ipsilaterally through tract DLV. d02 has smooth process in the GNG, wedge, vest, anterior ventral lateral protocerebrum and posterior ventral lateral protocerebrum, and varicose process in the wedge and GNG. d02 has dense innervation to the leg neuropils including the ventral association center (VAC), but avoids the dorsal part of the VNC, including neck motor, wing and haltere neuropils. A few processes project within the medial ventral association center. Axonal projections to the VNC return back into the posterior neck connective. The morphology is similar to an octopaminergic DN, termed the OA-VL1 (Busch et al., 2009).

(C-D) Morphology of DNd03. Whole cell morphology (C) and frontal sections of VNC are shown (D).

The cell body is located the GNG and the axon descends ipsilaterally through tract DLT. The DN has smooth process in the GNG, wedge, vest, anterior ventral lateral protocerebrum, posterior ventral lateral protocerebrum, saddle, flange, posterior lateral protocerebrum, and varicose process in the wedge and GNG. The morphology is similar to an octopaminergic DN, termed the OA-VL2 (Busch et al., 2009).

Figure 7—figure supplement 2

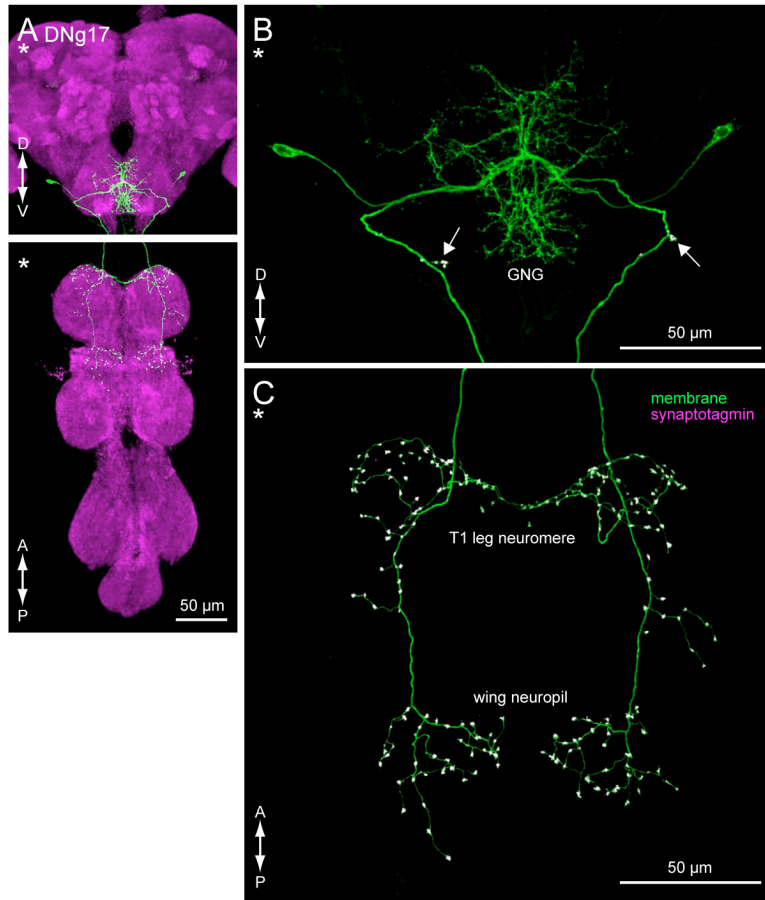


Figure 7. figure supplement 2. DN projecting to both wing and leg neuropil.

(A) DNg17 has smooth process in the saddle and GNG, and varicose process in the GNG. The DN descends contralaterally in the neck connective and projects to both leg and wing neuropils.

(B,C) Labeling of DNg17 with membrane (green) and presynaptic (magenta) markers in the brain (B) and VNC (C). The DN has a few process in the GNG, which show a positive signal for the presynaptic marker, and dense projections in the dorsal part of the prothoracic leg neuropil, and wing neuropil on the ipsilateral side.

Figure 7—figure supplement 3

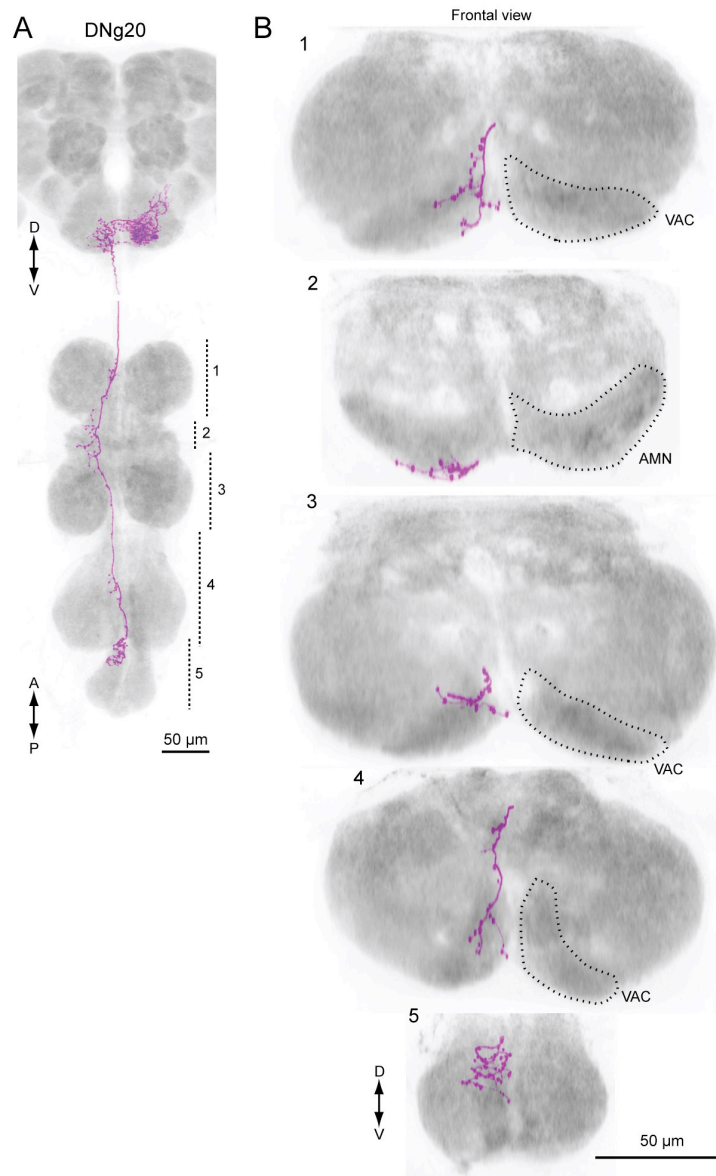


Figure 7. figure supplement 3. DN projecting to the ventral association center.

(A) Morphology of DNg20. The DN has smooth processes in the saddle and GNG, and smooth and varicose process in the GNG. The cell body is located on the GNG and the DN descends the contralateral neck connective.

(B) Frontal view of DNg20 innervation in the VNC. The number in the *top left* of each image corresponds to the number shown in the VNC in panel (A). The innervation is localized in the ventral most area of the VNC, which corresponds to the sensory area. The DN also projects to the accessory mesothoracic neuromere (AMN) (B2).

Figure 7—figure supplement 4

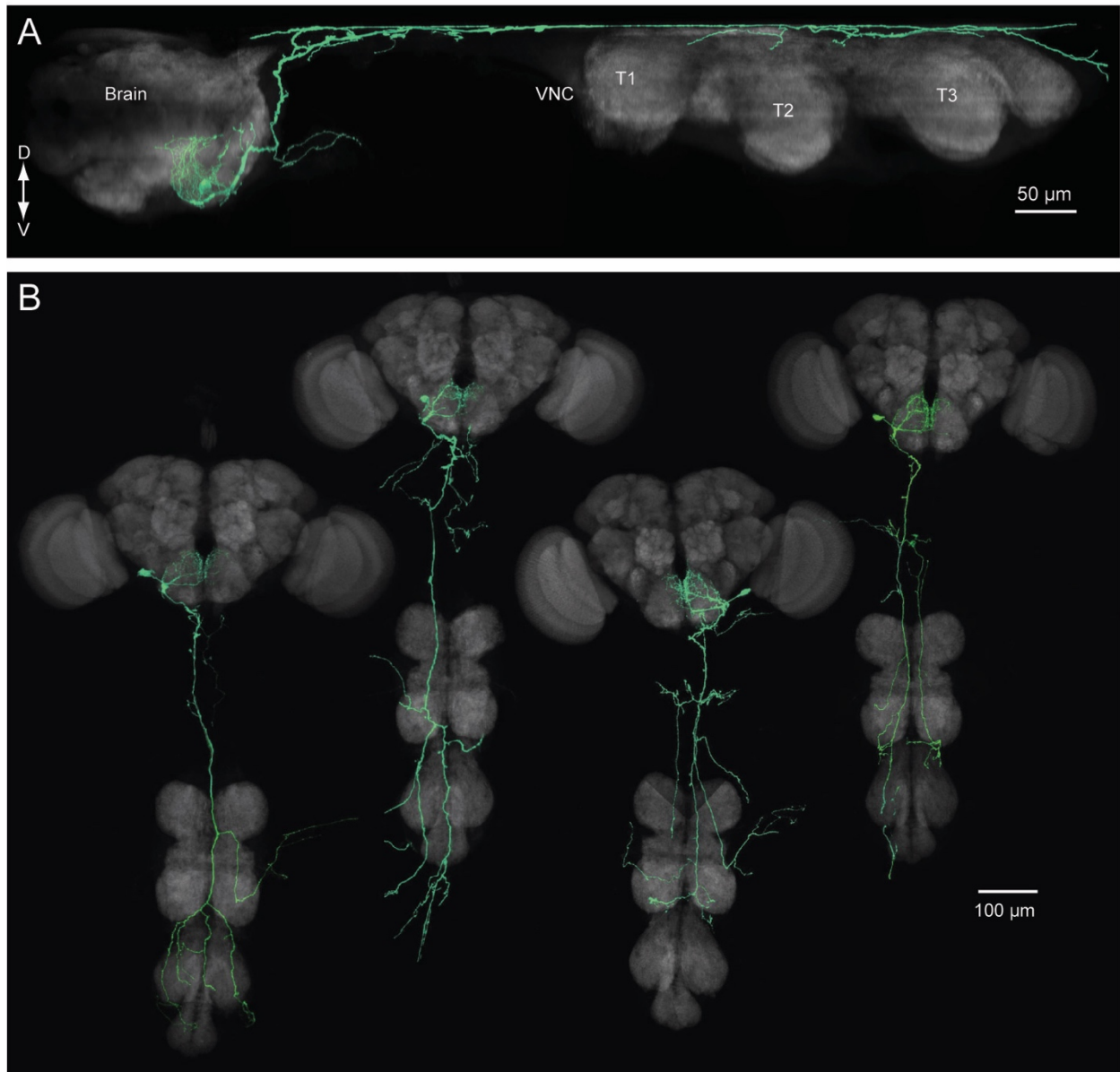


Figure 7. figure supplement 4. DN projecting outside the VNC.

(A) Lateral view of DNg28 morphology. The DN has smooth processes in the GNG, and varicose processes in the nerve fiber. The axon mainly runs through the dorsal surface of the VNC.

(B) Four examples of DNg28 morphology. The smooth processes in the brain are similar, whereas the axon pathways are highly variable.

Figure 9—figure supplement 1

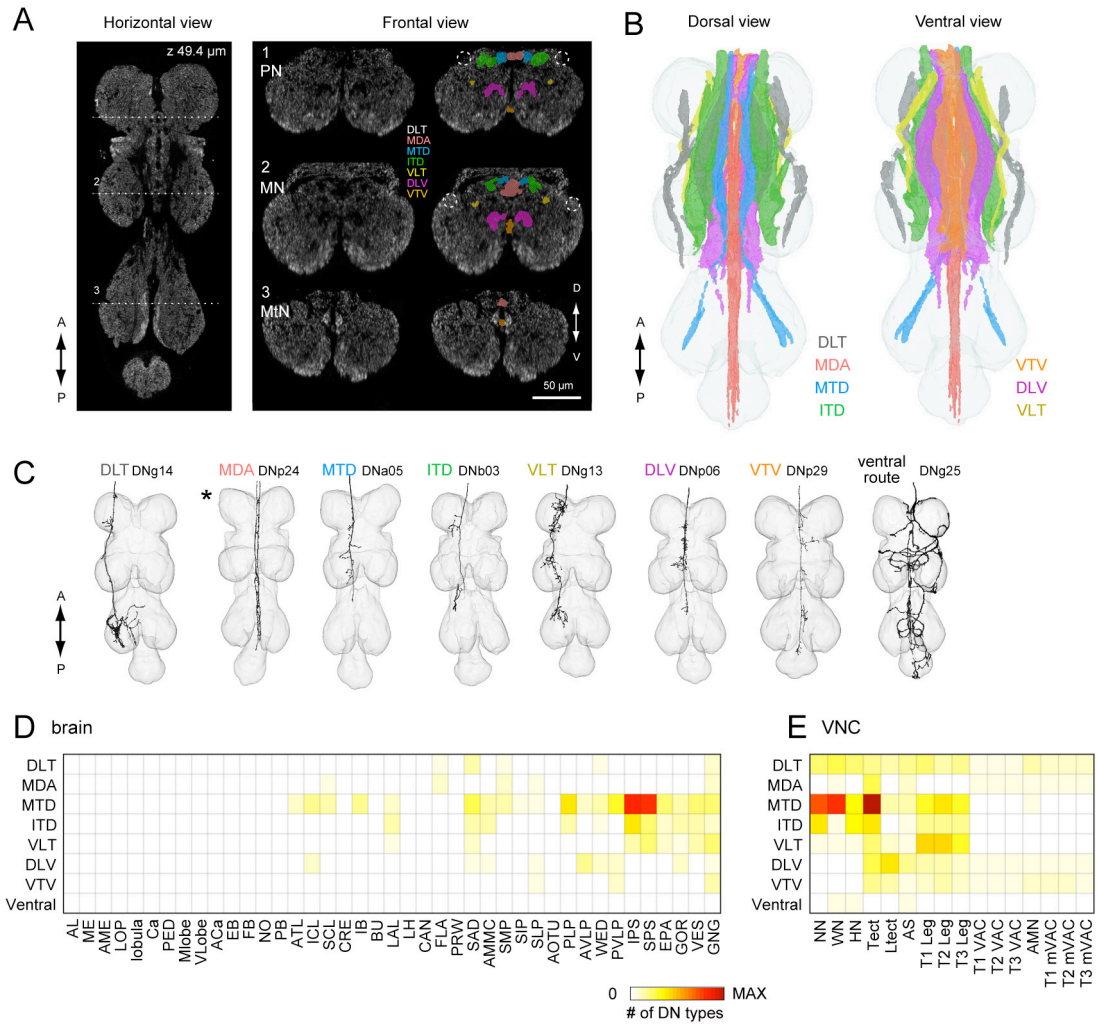


Figure 9. figure supplement 1. Neuronal pathways of DNs.

(A) Location of the DN tracts. Horizontal view of the whole VNC (*left*) and frontal sections of each segment are shown (*right*). Each frontal plane corresponds to the depth shown in dotted lines in the left panel. The tracts are labeled by color.

(B) Reconstruction of neuronal pathways in the VNC. Segmentation data used is from Boerner & Duch, 2010.

(C) Examples of DNs running through 8 different neuronal pathways. For each image, a DN on one side was reconstructed from confocal stacks.

(D-E) The relationship between the brain (D) or VNC (E) innervation and tract usage. The number of DN types are shown with pseudo-color.

Figure 10—figure supplement 1

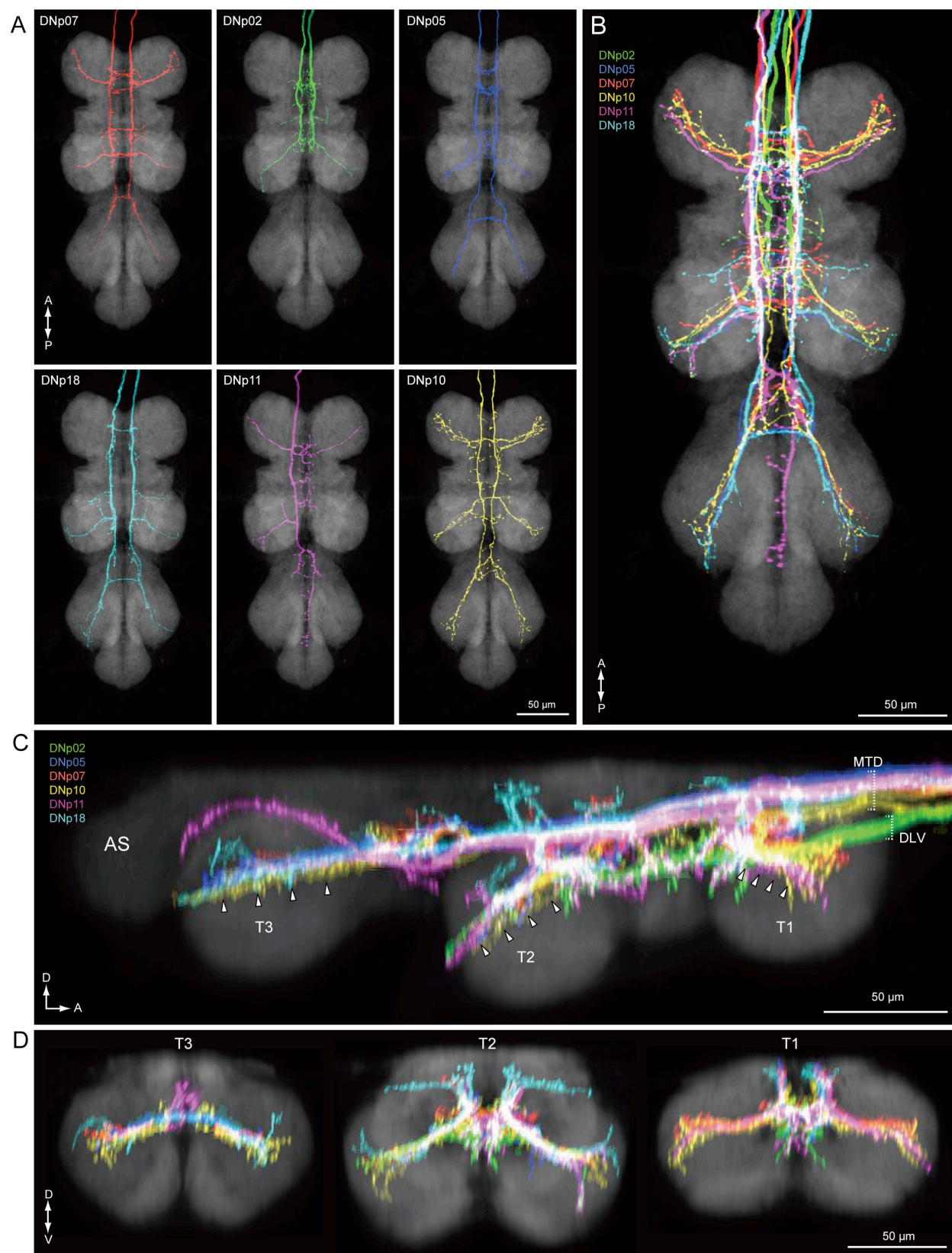


Figure 10. figure supplement 1. DNs running through the oblique tract.

(A) Morphologies of six DNs with axons in the oblique tract.

(B-D) Merged horizontal (B), sagittal (C), and frontal (D) views of the six DNs shown in panel (A), showing overlap and formation of the oblique tract. Individual data are compared by registration to a standard VNC. The DNs running through the MTD tract (DNp07, p05, p18, p11, and p10) run dorsally to the DN running through the DLV (DNp02).

Figure 10—figure supplement 2

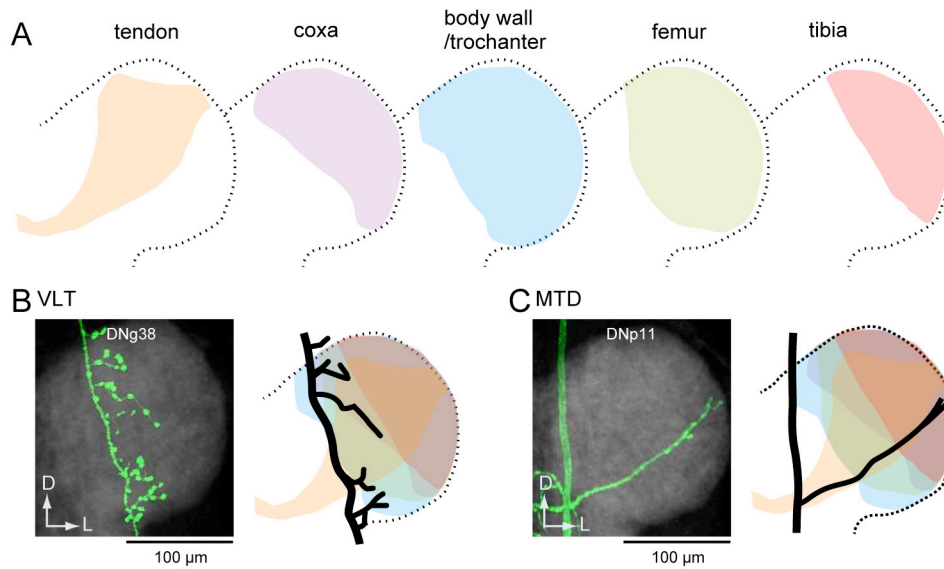


Figure 10. figure supplement 2. Potential overlap between DNs and leg motor neurons.

(A) Leg motor neuron dendrites form a myotopic map in each leg neuropil. Dendritic regions for motor neurons corresponding to different leg segments are schematized as different colored regions, based on Brierley et al., 2012.

(B) Axonal projection of DNg38 running through the VLT tract. Right panel shows potential overlap between the DN (black) and dendrites of leg motor neurons for proximal leg joints (color). The DN may not overlap with motor neurons for distal segments, such as tibia (red).

(C) Axonal projection of DNp11 running through the MTD and oblique tracts. Left panels shows potential overlap between the DN (black) and dendrites of leg motor neurons (color). The DN may overlap leg motor neurons for all segments.

Figure 11—figure supplement 1

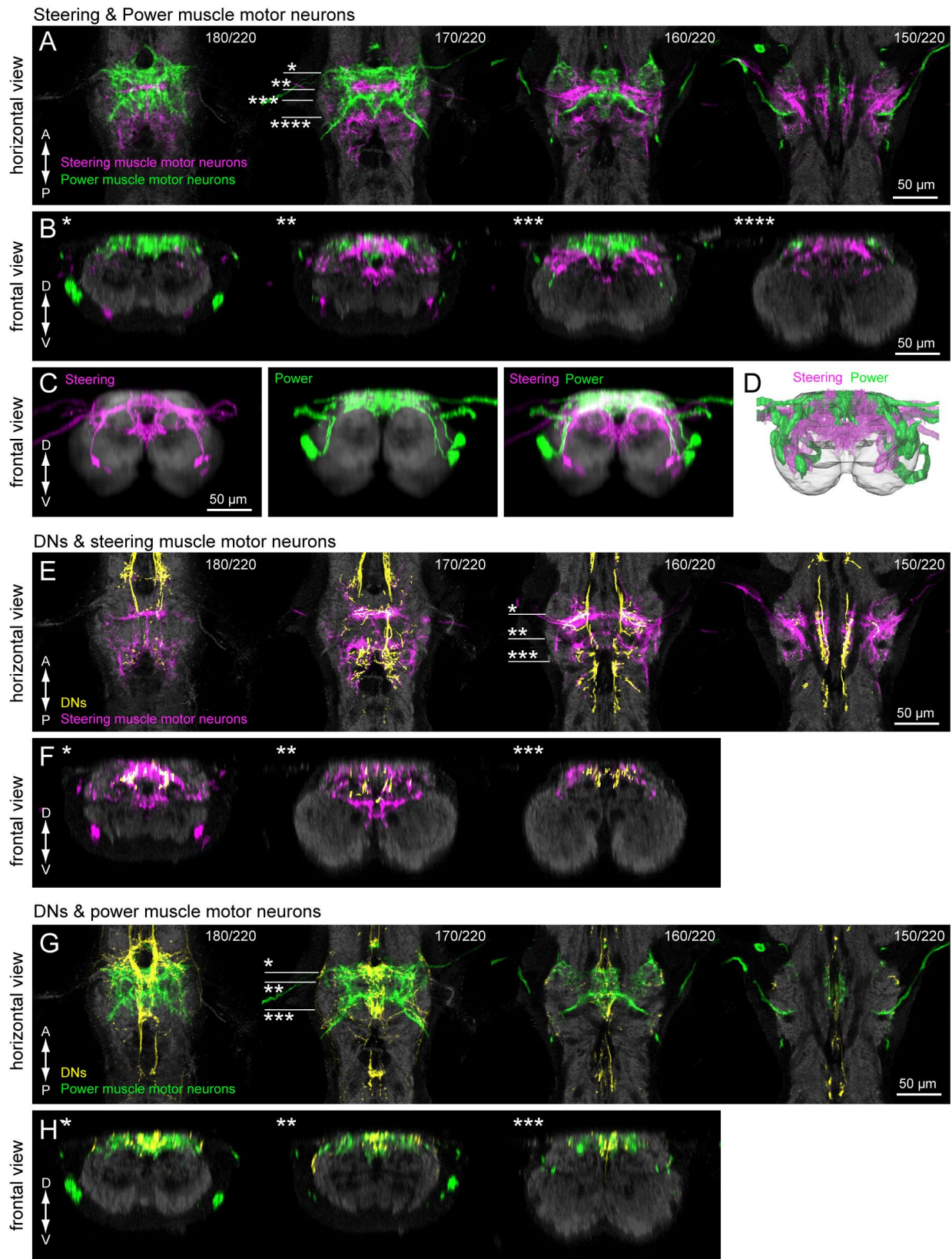


Figure 11. figure supplement 1. Innervation in the wing neuropil of DNs and interneurons.

(A,B) Confocal stacks of power muscle (green) and steering muscle (magenta) motor neurons (MNs). horizontal (A) and frontal (B) views are shown. For each image, the depth of the horizontal plane is shown in the *top-right* (A). The depth in anterior-posterior axis shown in (B) corresponds to the line markers shown in (A). The innervation profile of power and steering MNs is largely segregated.

(C) Maximum intensity projection of T2 segment for steering muscle MNs (*left*), power muscle MNs (*center*) and both with counterstaining (*right*).

(D) Three-dimensional reconstruction of dendritic innervation of power and steering muscle motor neurons.

(E,F) Confocal stacks of steering muscle MNs (magenta) and a group of type-I DNs (yellow). Horizontal (E) and frontal views are shown (F).

(G,H) Confocal stacks of populations of power muscle motor neurons (green) and a population of type-II DNs (yellow). Dorsal (G) and frontal (H) views are shown.

Figure 11—figure supplement 2

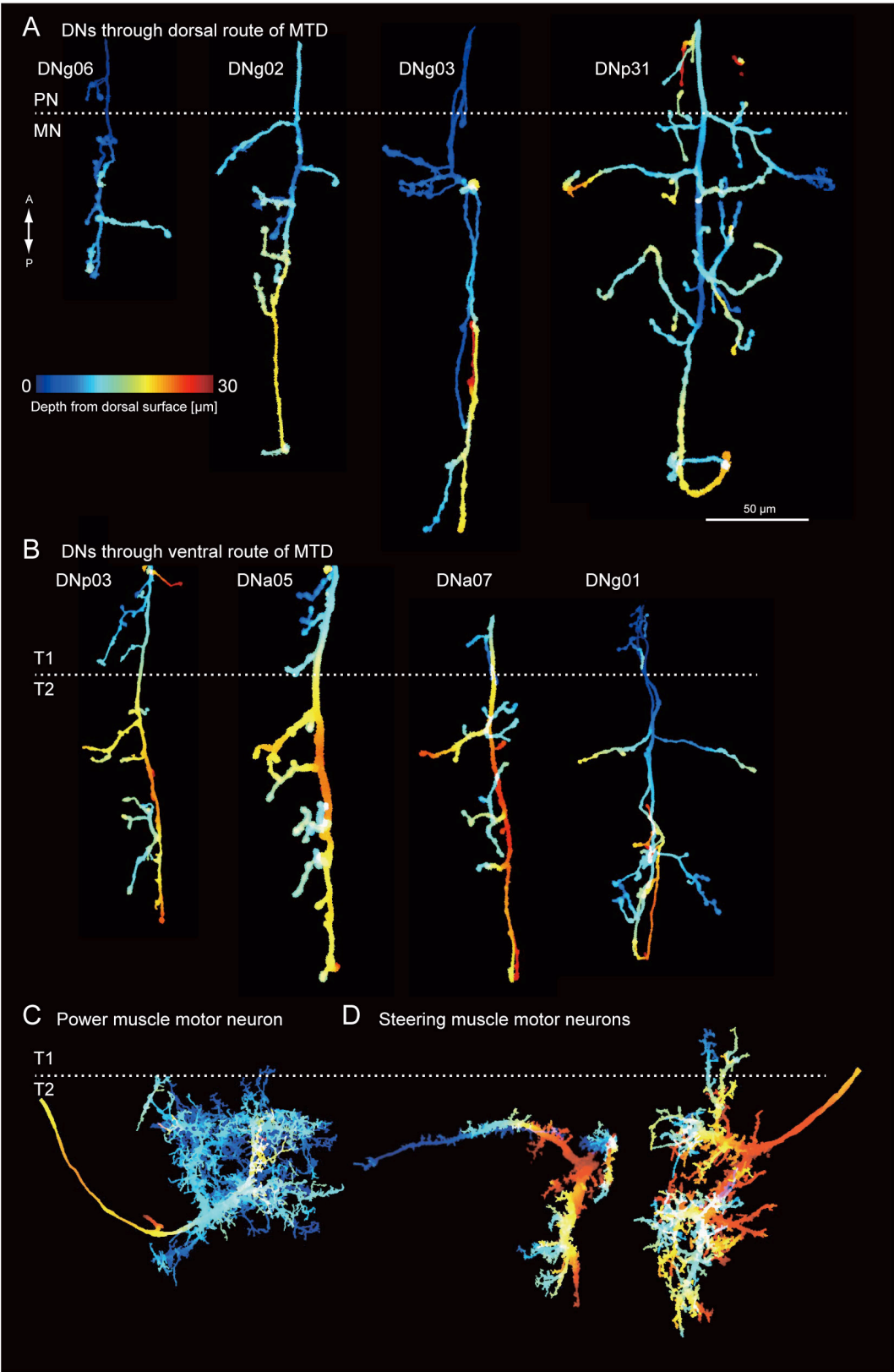


Figure 11. figure supplement 2. Innervation in the wing neuropil of DNs and interneurons.

(A) Reconstructed morphology of four different DNs running through the dorsal route of the MTD shown with pseudo-color for depth. Cold and hot colors indicate the dorsal and ventral part of the wing neuropil, respectively.

(B) As in (A) for four DNs running through the ventral route of the MTD. The anteriormost branch mostly shows wider innervation, which is located deeper than those in DNs through dorsal tract of the MTD (A).

(C) As in (A) for a power muscle MN for the dorsoventral muscle.

(D) As in (A) for steering muscle MNs for basalar 1 (*left*) and 2 (*right*).

Figure 12—figure supplement 1

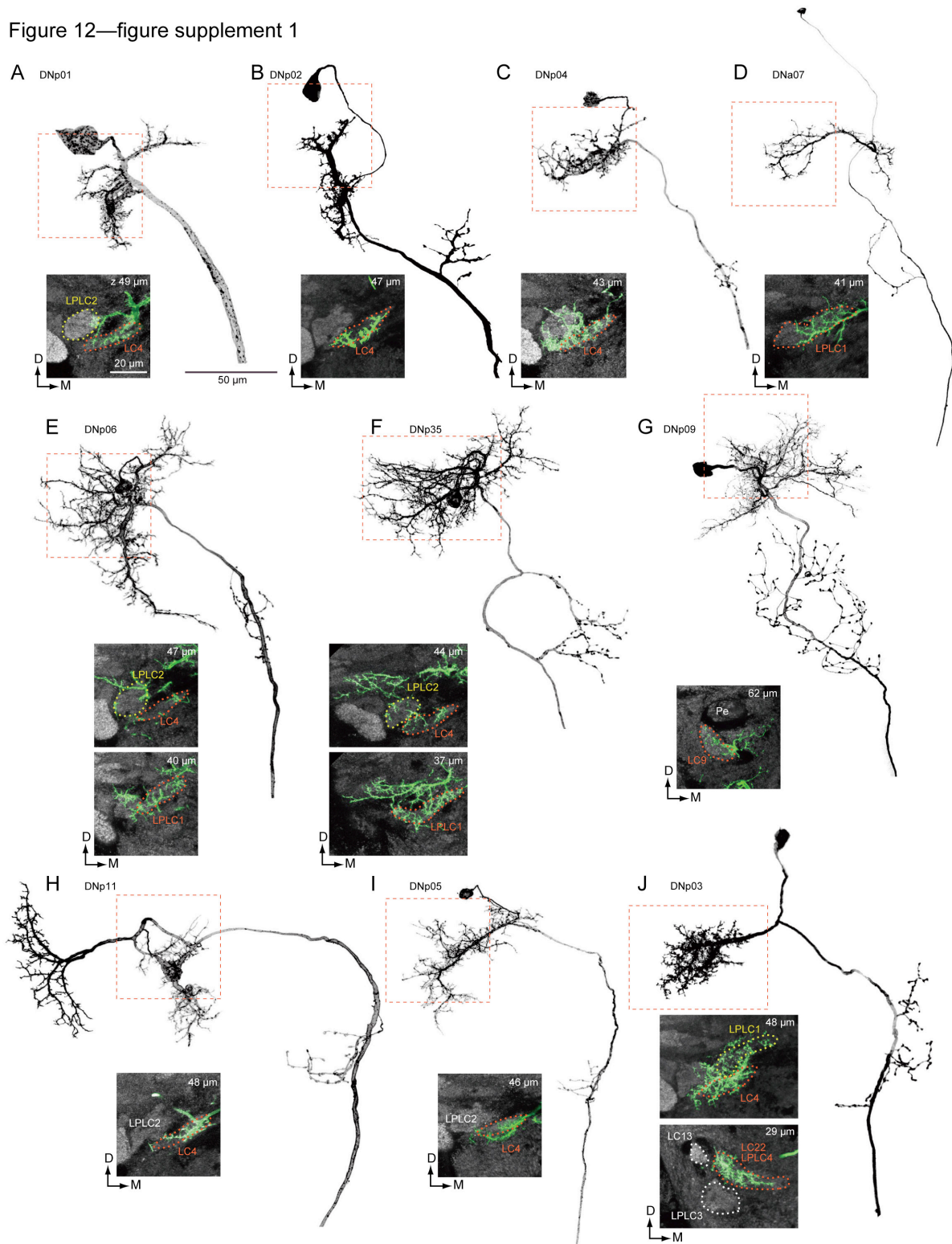


Figure 12. figure supplement 1. Morphology of DNs from optic glomeruli in the posterior ventral protocerebrum.

High resolution (63x) confocal images of the 10 different DNs innervating the optic glomeruli in the PVLP. Neurite morphology in the brain is shown, as well as images at the depth of the optic glomeruli (*insets*). Seven DNs descend on the ipsilateral side and the others descend on the contralateral side. DNs have smooth process in one or a few optic glomeruli and most of DNs (9 out of 10) have varicose process in the GNG. DN cell membrane, green; NC82 neuropil stain, grey; yellow and red dotted circles indicate individual glomeruli.

Figure 12—figure supplement 2

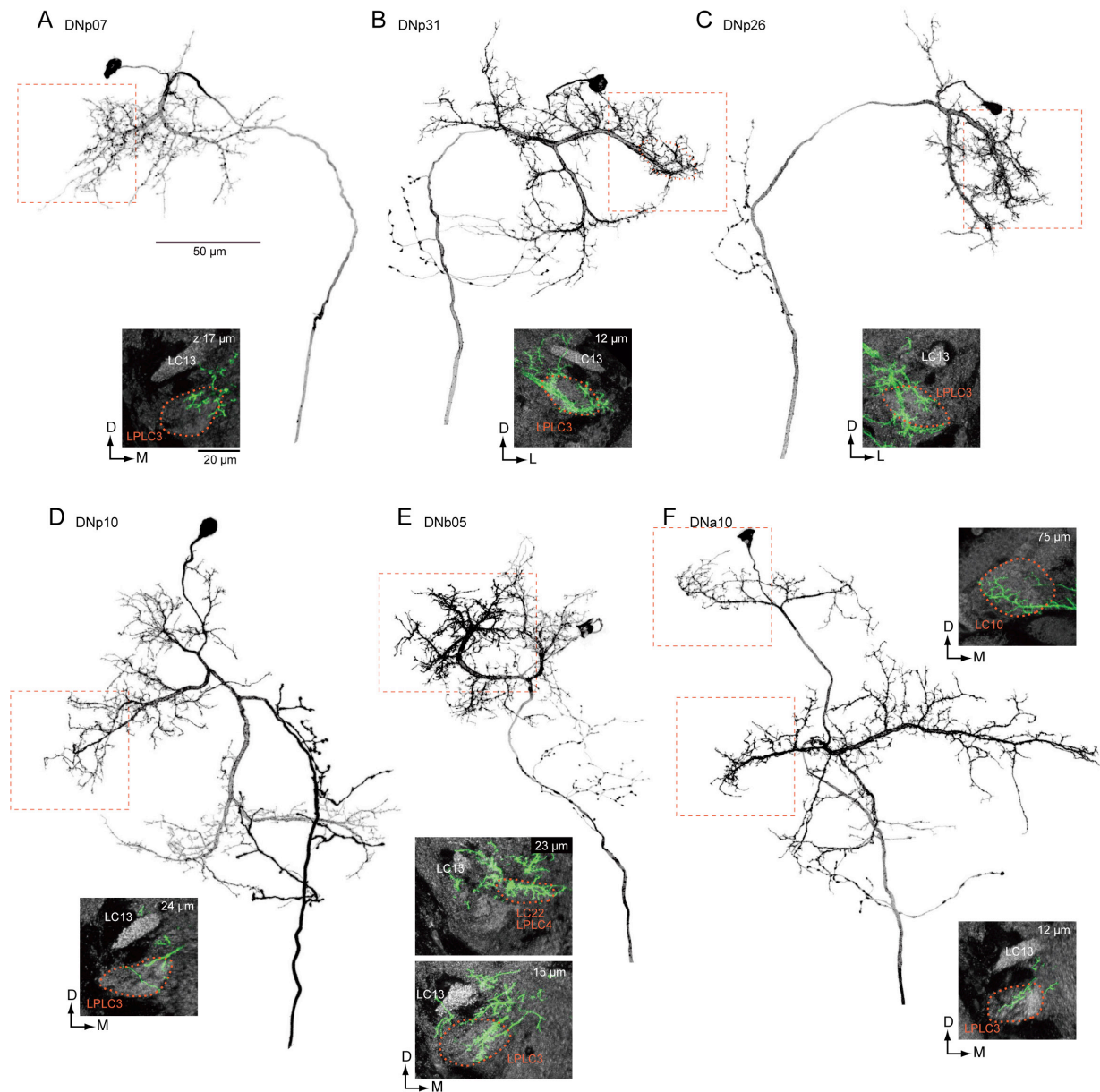


Figure 12. figure supplement 2. Morphology of DNs from optic glomeruli in the posterior lateral protocerebrum.

High resolution (63x) confocal images of the six different DNs innervating the PLP optic glomeruli.

Images as in Figure 10. The majority of these DNs (5 out of 6) descend contralaterally through the neck connective.

Figure 12—figure supplement 3

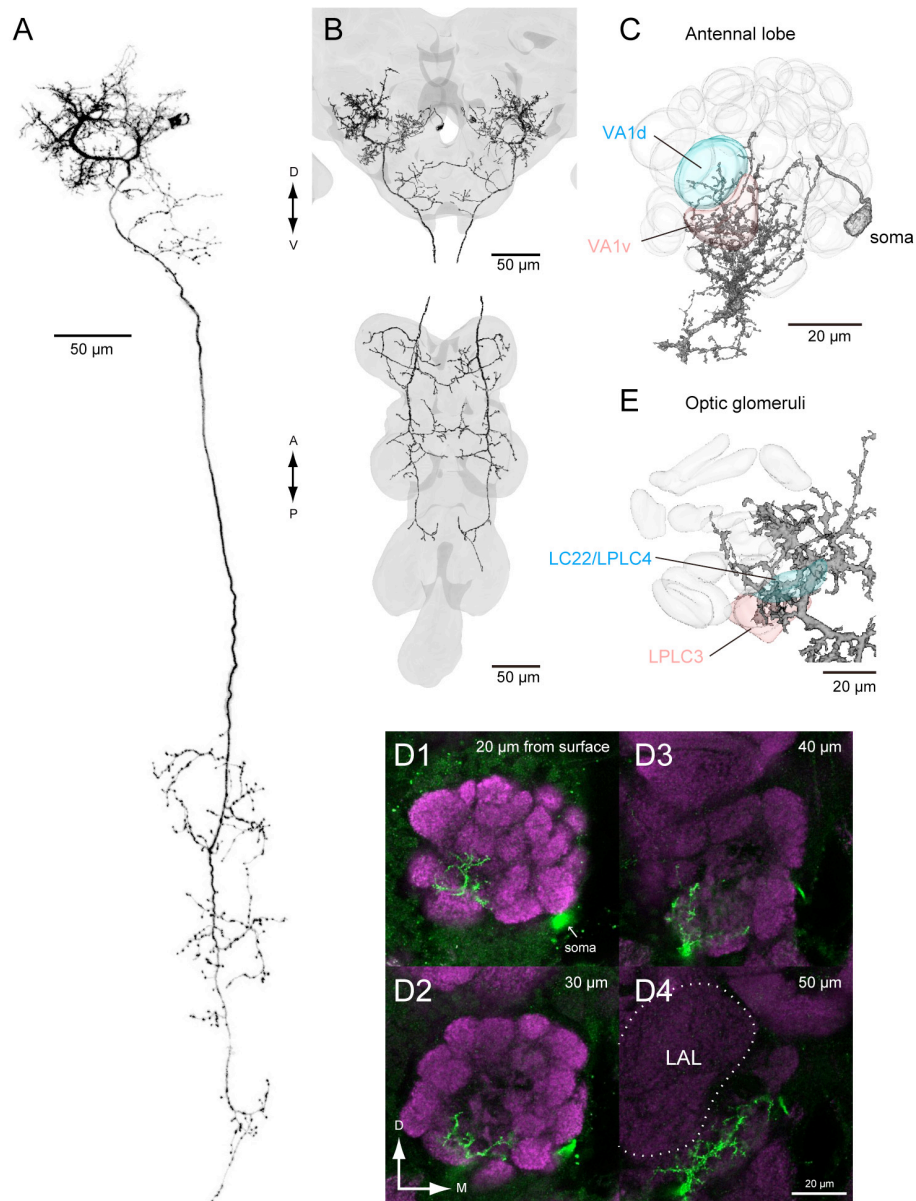


Figure 12. figure supplement 3. Morphology of a DN innervating both olfactory and optic glomeruli.

(A) Morphology of DNb05.

(B) Segmentation of DNb05 on both sides. The outer shapes of the brain and VNC are shown with gray.

(C) Reconstruction of DN innervation in the antennal lobe. Neuron and glomeruli are shown in black and gray, respectively. The glomeruli innervated by the DN are shown in color.

(D) Confocal stacks of DN innervation in the antennal lobe. Plane depth indicated in *top-right* of images.

(E) Reconstruction of DN innervation to the optic glomeruli. Colors as in (C)

Name	Similar neuron	Citation
DNa01	aSP3 VGlut-F-200324	Yu et al., 2010 FlyCircuit
DNa05	DNDC 2-2	Gronenberg & Strausfeld, 1992
DNa10	VGlut-F-200121	FlyCircuit
DNb01	VGlut-F-500726	FlyCircuit
DNb02	fru-F-100073, VGlut-F-300245	FlyCircuit
DNb05	T1 AMMC-Di7	Stocker et al., 1990 Matsuo et al., 2016
DNd01	fru-F-500429	FlyCircuit
DNd02	OA-VL1	Busch et al., 2009
DNd03	OA-VL2	Busch et al., 2009
DNg07	aPN VGlut-F-500136	Vaughan et al., 2014 FlyCircuit
DNg08	VGlut-F-400822	FlyCircuit
DNg12	aDN1	Hampel et al., 2015
DNg13	pSG3	Yu et al., 2010
DNg15	AMMC-Db5	Matsuo et al., 2016
DNg16	VGlut-F-600012, VGlut-F-200371	FlyCircuit
DNg25	one of CCAP	Lee et al. 2013, Fig1G
DNg26	aSG3 fru-F-900021 one neuron in hugS3-GAL4	Yu et al., 2010 FlyCircuit Melcher & Pankratz, 2005
DNg28	2 large cell in TRH-Gal4	Alekseyenko et al., 2010
DNg29	AMMC-Db7	Matsuo et al., 2016
DNg30	ICLI	Jiang et al., 2013
DNg31	fru-F-000167	FlyCircuit
DNg34	OA-VPM1/aDT8	Busch et al., 2009; Yu et al., 2010
DNg38	Gad1-F-500376	FlyCircuit
DNg39	VGlut-F-300006, Gad1-F-000424	FlyCircuit
DNp01	giant descending neuron	Milde & Strausfeld, 1990
DNp02	lateral giant P3b	Milde & Strausfeld, 1990 Kimura et al., 2008
DNp03	Cha-F-200252	FlyCircuit
DNp04	Ipsilateral small neuron	Milde & Strausfeld, 1990
DNp05	contralateral giant mimetics Vglut-F-500311 AMMC-Db2	Milde & Strausfeld, 1990 FlyCircuit Matsuo et al., 2016
DNp06	Inferior giant AMMC-Di5	Milde & Strausfeld, 1990 Matsuo et al., 2016
DNp08	VGlut-F-500767	FlyCircuit
DNp11	LDN AMMC-Db3	Nässel & Strausfeld, 1982 Matsuo et al., 2016
DNp13	fru-F-800097	FlyCircuit
DNp14	VGlut-F-300326	FlyCircuit
DNp15	VGlut-F-800293, Cha-F-700077 DNHS1	FlyCircuit Suver et al., 2016
DNp16	PSp2 (neuroblast)	Ito et al., 2013
DNp17	PSp2 (neuroblast)	Ito et al., 2013
DNp18	VGlut-F-200226, fru-F-700251	FlyCircuit
DNp20	DNOVS1	Strausfeld & Bassemir, 1985
DNp22	DNOVS2 or DNOVS3 VGlut-F-500165, VGlut-F-200420	Strausfeld & Bassemir, 1985 FlyCircuit
DNp23	Cha-F-100034	FlyCircuit
DNp24	E0585-F-200004	FlyCircuit
DNp29	SP1	Nässel, 1993
DNp30	GAMDN	Mu et al., 2014
DNp32	AL-DN1	Tanaka et al., 2012
DNp33	AMMC D1	Matsuo et al., 2014
DNx01	large campaniform cell	Nässel et al., 1984

Supplementary Table 2. Descending neurons with similar morphology reported in *Drosophila melanogaster* and other species.

Full references listed below in “Additional references for Supplementary Table 2.”

Robot ID	LineName	Genotype stock name	DN type	quality
3018528	SS02536	BJD_111C04_BB_21-x-BJD_126F02_AV_01	DNa05	A
3016845	SS01546	BJD_111C04_BB_21-x-BJD_104E03_AV_01	DNa05, DNa07	A
3016859	SS01560	GMR_31H10_XA_21-x-BJD_111C04_AV_01	DNa07	A
3018296	SS02393	BJD_104B12_BB_21-x-GMR_80H02_AV_01	DNa08	A
3018272	SS02370	GMR_55D12_XA_21-x-GMR_72H04_XD_01	DNb03	A
3018544	SS02552	GMR_55D12_XA_21-x-BJD_119B11_AV_01	DNb03	A
3015812	SS01051	BJD_113B12_BB_21-x-BJD_110E05_AV_01	DNb05	A
3018681	SS02631	GMR_20C04_XA_21-x-BJD_113E03_AV_01	DNb06	A
3020785	SS04161	GMR_59A06_XA_21-x-GMR_64B11_XD_01	DNc01	A
3016869	SS01570	BJD_103G03_BB_21-x-BJD_121A10_AV_01	DNd02, DNd03	A
3017890	SS02111	BJD_119A05_BB_21-x-BJD_105G01_AV_01	DNg10	A
3016846	SS01547	BJD_111G08_BB_21-x-BJD_105G01_AV_01	DNg10	A
3016878	SS01579	BJD_113G07_BB_21-x-GMR_81C11_XD_01	DNg11	A
3018530	SS02538	BJD_118A10_BB_21-x-BJD_123E03_AV_01	DNg01	A
3018151	SS02285	BJD_114G06_BB_21-x-BJD_121E05_AV_01	DNg01	A
3015830	SS01069	GMR_38H06_XA_21-x-BJD_104A09_AV_01	DNg14	A
3020782	SS04158	GMR_53D12_XA_21-x-BJD_104A09_AV_01	DNg14	A
3018145	SS02279	BJD_137F08_BB_21-x-BJD_119H02_AV_01	DNg17	A
3013808	SS00898	BJD_137F08_BB_21-x-BJD_103G08_AV_01	DNg17	A
3018675	SS02625	BJD_111B02_BB_21-x-BJD_110C03_AV_01	DNg02	A
3015807	SS01046	BJD_105D02_BB_21-x-GMR_24C07_XD_01	DNg24	A
3015813	SS01052	BJD_122B03_BB_21-x-GMR_22D06_XD_01	DNg25	A
3015820	SS01059	GMR_21F01_XA_21-x-GMR_22D06_XD_01	DNg25	A
3016857	SS01558	GMR_27E07_XA_21-x-BJD_109H06_AV_01	DNg26	A
3016856	SS01557	GMR_13D04_XA_21-x-GMR_65D05_XD_01	DNg27	A
3020783	SS04159	GMR_59F08_XA_21-x-GMR_47H03_XD_01	DNg29	A
3018540	SS02548	GMR_42B02_XA_21-x-BJD_119F07_AV_01	DNg03	A
3018281	SS02378	GMR_61A01_XA_21-x-GMR_13B05_XD_01	DNg30	A
3018291	SS02388	GMR_14H09_XA_21-x-GMR_61A01_AW_01	DNg30	A
3015815	SS01054	GMR_14H09_XA_21-x-GMR_56H09_XD_01	DNg30	A
3015838	SS01077	GMR_61A01_XA_21-x-BJD_102G11_AV_01	DNg30	A
3018182	SS02316	GMR_14H09_XA_21-x-BJD_127A06_AV_01	DNg30	A
3018316	SS02324	GMR_42B02_XA_21-x-BJD_127F10_AV_01	DNg07	A
3015835	SS01074	GMR_42B02_XA_21-x-GMR_89B01_XD_01	DNg07	A
3016896	SS01597	GMR_42B02_XA_21-x-BJD_101D01_AV_01	DNg07	A
3018539	SS02547	GMR_42B02_XA_21-x-BJD_119A06_AV_01	DNg07	A
3018546	SS02554	GMR_73A05_BB_21-x-BJD_119A06_AV_01	DNg07	A
3018685	SS02635	GMR_42B02_XA_21-x-BJD_129H09_AV_01	DNg07, DNg08	A
3018165	SS02299	GMR_10A12_XA_21-x-BJD_125A05_AV_01	DNp01	A
3016907	SS01608	GMR_94E01_XA_21-x-BJD_115F05_AV_01	DNp10	A
3018288	SS02385	GMR_94E01_XA_21-x-GMR_48E11_XD_01	DNp10	A
3015810	SS01049	BJD_110A11_BB_21-x-BJD_115F05_AV_01	DNp10	A
3016879	SS01580	BJD_115F05_BB_21-x-GMR_48E11_XD_01	DNp10	A
3015839	SS01078	GMR_69C11_XA_21-x-GMR_81D05_XD_01	DNp20	A
3015817	SS01056	GMR_17A04_XA_21-x-GMR_24A03_XD_01	DNp27	A
3016888	SS01589	GMR_20C03_XA_21-x-GMR_23C07_XD_01	DNp27	A
3018652	SS02618	GMR_11H10_XA_21-x-BJD_104H02_AV_01	DNp28	A
3016895	SS01596	GMR_29F12_XA_21-x-GMR_37G07_XD_01	DNp03	A
3018290	SS02387	GMR_60B12_XA_21-x-GMR_58E05_XD_01	DNp04	A
3015841	SS01080	GMR_84B12_XA_21-x-BJD_105D02_AV_01	DNp04	A
3016843	SS01544	BJD_105D02_BB_21-x-BJD_124C05_AV_01	DNp04, DNp02	A
3018158	SS02292	BJD_107A06_BB_21-x-BJD_124C05_AV_01	DNp04, DNp06	A
3018122	SS02256	BJD_107A12_BB_21-x-BJD_107A06_AV_01	DNp06	A
3018142	SS02276	BJD_113F07_BB_21-x-BJD_118E07_AV_01	DNp07	A
3016839	SS01540	BJD_104B12_BB_21-x-GMR_38F04_XD_01	DNp09	A
3018176	SS02310	BJD_118E07_BB_21-x-BJD_126F02_AV_01	several types of DNa DNs	A
3007652	SS00731	GMR_22C05_XA_21-x-GMR_56G08_XD_01	DNa01	B
3007651	SS00730	GMR_75C10_XA_21-x-GMR_87D07_XD_01	DNa02	B
3018287	SS02384	BJD_118E07_BB_21-x-GMR_47D05_AV_01	DNa04, DNa10	B
3016851	SS01552	BJD_115A02_BB_21-x-BJD_111C04_AV_01	DNa05, DNa7	B
3016871	SS01572	BJD_105D02_BB_21-x-BJD_100H09_AV_01	DNa05, DNp11	B
3016840	SS01541	BJD_104E03_BB_21-x-GMR_56G08_XD_01	DNa07	B
3016841	SS01542	BJD_104E03_BB_21-x-GMR_87B09_XD_01	DNa07	B
3016870	SS01571	BJD_104E03_BB_21-x-BJD_100E01_AV_01	DNa07	B
3018286	SS02383	BJD_103G04_BB_21-x-GMR_45H03_AV_01	DNb01	B
3018534	SS02542	BJD_144E04_BB_21-x-BJD_103G04_AV_01	DNb01	B
3018299	SS02396	GMR_21F05_XA_21-x-GMR_93B10_AV_01	DNb02	B
3016899	SS01600	GMR_59B10_XA_21-x-GMR_21F05_XD_01	DNb02	B

Supplementary Table 3. Continued on next page.

3015821	SS01060	GMR_21F05_XA_21-x-GMR_21H11_XD_01	DNb02	B
3018298	SS02395	BJD_120G05_BB_21-x-GMR_83B06_AV_01	DNc02	B
3016844	SS01545	BJD_109D01_BB_21-x-BJD_102A03_AV_01	DNd02	B
3016874	SS01575	BJD_109D01_BB_21-x-BJD_120E12_AV_01	DNd02	B
3016868	SS01569	BJD_103G03_BB_21-x-BJD_111F03_AV_01	DNd02, DNd03	B
3016875	SS01576	BJD_109D01_BB_21-x-GMR_70C05_XD_01	DNd02, DNd03	B
3018144	SS02278	BJD_111G08_BB_21-x-BJD_119A05_AV_01	DNg10	B
3018294	SS02391	GMR_81C11_XA_21-x-GMR_66B05_AV_01	DNg11	B
3016849	SS01550	BJD_113G07_BB_21-x-BJD_126F01_AV_01	DNg11	B
3016865	SS01566	GMR_66B05_XA_21-x-GMR_85H06_AV_01	DNg11	B
3018651	SS02617	BJD_129H09_BB_21-x-BJD_126F01_AV_01	DNg11	B
3018643	SS02609	BJD_113D11_BB_21-x-BJD_113F09_AV_01	DNg12	B
3018642	SS02608	BJD_113D11_BB_21-x-BJD_113E03_AV_01	DNg12	B
3018125	SS02259	BJD_117F04_BB_21-x-BJD_109F06_AV_01	DNg13	B
3016866	SS01567	GMR_88F03_XA_21-x-BJD_109F06_AV_01	DNg13	B
3018141	SS02275	BJD_122H12_BB_21-x-BJD_118A10_AV_01	DNg01	B
3016864	SS01565	GMR_60B11_XA_21-x-GMR_83B04_XD_01	DNg01	B
3018280	SS02377	BJD_105A09_BB_21-x-BJD_127H02_AV_01	DNg15	B
3016842	SS01543	BJD_105A07_BB_21-x-BJD_107F12_AV_01	DNg16	B
3018674	SS02624	BJD_110C03_BB_21-x-BJD_111B02_AV_01	DNg02	B
3018684	SS02634	GMR_42B02_XA_21-x-BJD_118C08_AV_01	DNg02	B
3015834	SS01073	GMR_42B02_XA_21-x-GMR_65C10_XD_01	DNg02	B
3016860	SS01561	GMR_42B02_XA_21-x-BJD_106G05_AV_01	DNg02	B
3007653	SS00732	GMR_14F03_XA_21-x-GMR_24C07_XD_01	DNg24	B
3016901	SS01602	GMR_64B03_XA_21-x-GMR_29G08_XD_01	DNg25	B
3013833	SS00923	BJD_109B01_BB_21-x-BJD_104F07_AV_01	DNg26	B
3018123	SS02257	GMR_10A07_XA_21-x-BJD_109B01_AV_01	DNg26	B
3015822	SS01061	GMR_22H02_XA_21-x-GMR_20F03_XD_01	DNg26	B
3015825	SS01064	GMR_27E07_XA_21-x-GMR_14D01_XD_01	DNg26	B
3016892	SS01593	GMR_27E07_XA_21-x-GMR_20F03_XD_01	DNg26	B
3015824	SS01063	GMR_24F06_BB_21-x-GMR_45E06_XD_01	DNg28	B
3016863	SS01564	GMR_44A07_XA_21-x-BJD_114C04_AV_01	DNg28	B
3015836	SS01075	GMR_47H03_XA_21-x-GMR_59F08_XD_01	DNg29	B
3018683	SS02633	GMR_42B02_XA_21-x-BJD_102B12_AV_01	DNg03	B
3016887	SS01588	GMR_14H09_XA_21-x-GMR_13B05_XD_01	DNg30	B
3016852	SS01553	BJD_119E05_BB_21-x-GMR_89A03_XD_01	DNg30	B
3016903	SS01604	GMR_73A05_XA_21-x-BJD_100F04_AV_01	DNg07	B
3007648	SS00727	GMR_14A01_XA_21-x-GMR_79H02_XD_01	DNp01	B
3007647	SS00726	GMR_25C08_XA_21-x-GMR_68A06_XD_01	DNp01	B
3018963	SS02891	BJD_110D01_BB_21-x-BJD_105F11_AV_01	DNp11	B
3016855	SS01556	GMR_11E07_XA_21-x-GMR_77F05_AV_01	DNp15	B
3007656	SS00735	GMR_49A07_XA_21-x-GMR_55A03_XD_01	DNp16	B
3018545	SS02553	GMR_67E08_XA_21-x-BJD_137F12_AV_01	DNp17	B
3018295	SS02392	BJD_119C06_BB_21-x-GMR_69C11_XD_01	DNp18	B
3015814	SS01053	BJD_124F08_BB_21-x-GMR_24A03_XD_01	DNp02	B
3016853	SS01554	BJD_124F08_BB_21-x-BJD_124C05_AV_01	DNp02	B
3018282	SS02379	BJD_110D01_BB_21-x-GMR_15E12_AV_01	DNp02, DNp11	B
3018526	SS02534	BJD_110D01_BB_21-x-BJD_124C05_AV_01	DNp02, DNp11	B
3007650	SS00729	GMR_58G11_XA_21-x-GMR_81D05_XD_01	DNp20	B
3015818	SS01057	GMR_20C05_XA_21-x-GMR_85H06_AV_01	DNp20	B
3016889	SS01590	GMR_20C03_XA_21-x-GMR_31B08_XD_01	DNp27	B
3016886	SS01587	GMR_11H10_XA_21-x-BJD_104F07_AV_01	DNp28	B
3015827	SS01066	GMR_30C12_XA_21-x-GMR_22D06_XD_01	DNp03	B
3015842	SS01081	GMR_91C05_XA_21-x-GMR_31B08_XD_01	DNp03	B
3016858	SS01559	GMR_29F12_XA_21-x-GMR_88C07_XD_01	DNp03	B
3018285	SS02382	GMR_91C05_XA_21-x-GMR_37G07_XD_01	DNp03	B
3018297	SS02394	GMR_61H01_XA_21-x-GMR_82C10_AV_01	DNp32	B
3013846	SS00934	BJD_127A08_BB_21-x-BJD_105D02_AV_01	DNp04	B
3007646	SS00725	GMR_50D07_XA_21-x-GMR_33H11_XD_01	DNp04	B
3013775	SS00865	BJD_104B02_BB_21-x-BJD_103C12_AV_01	DNp05	B
3015808	SS01047	BJD_107A12_BB_21-x-BJD_124C05_AV_01	DNp06	B
3018646	SS02612	BJD_118E07_BB_21-x-BJD_103C12_AV_01	DNp07	B
3016848	SS01549	BJD_113F07_BB_21-x-BJD_103C12_AV_01	DNp07, DNp13	B
3016881	SS01582	BJD_117H04_BB_21-x-BJD_114A11_AV_01	DNb04	C
3016880	SS01581	BJD_116F08_BB_21-x-BJD_102D12_AV_01	DNp13, DNp29	C
3015823	SS01062	GMR_24A03_XA_21-x-GMR_74C01_XD_01	Empty brain control	A

Supplementary Table 3. DN Split-GAL4 lines generated and used in this study.

Quality A, sparse lines without background expression; Quality B, lines with a few background expression; Quality C, lines with background expression.

Citation	Cell type	Robot ID	LineName	Split pair
Fig 4-S1 A	mnb1	3021403	SS04528	GMR_16E11_XA_21-x-GMR_21C11_XD_01
Fig 4-S1 B	mnb2	3007658	SS00737	GMR_10A12_XA_21-x-GMR_81E05_XD_01
Fig 4-S1 C	DVM	3007658	SS00737	GMR_10A12_XA_21-x-GMR_81E05_XD_01
Fig 4-S1 D	interneuron	3021403	SS04528	GMR_16E11_XA_21-x-GMR_21C11_XD_01
Fig 4-S1 E	interneuron	3025428	SS31976	GMR_18A05_BB_21-x-BJD_111F03_AV_01
Fig 4-S2 A	TTMn	3018673	SS02623	BJD_110A03_BB_21-x-BJD_103B10_AV_01
Fig 4-S2 B	PSI	3003982	VT049105	-
Fig 4-S2 C	interneuron	3003982	VT049105	-
Fig 4-S2 D	interneuron	3018678	SS02628	BJD_119F12_BB_21-x-BJD_127F04_AV_01
Fig 4-S2 E	III1mn	3016891	SS01592	GMR_26E02_XA_21-x-GMR_81D05_XD_01

Supplementary Table 4. Inter- and motor neuron split-GAL4 lines generated in this study.

Robot ID	LineName	Genotype stock name	DN type	quality
3007645	SS00724	GMR_31B08_XA_21-x-GMR_24A03_XD_01	DNp03, DNp28, DNp02	C
3007649	SS00728	GMR_25C08_XA_21-x-GMR_79H02_XD_01	DNp01	C
3007654	SS00733	GMR_58E07_XA_21-x-GMR_39H12_XD_01	DNp31	C
3007655	SS00734	GMR_73C04_XA_21-x-GMR_39H12_XD_01	DNb05	C
3007657	SS00736	GMR_21A07_XA_21-x-GMR_72A01_XD_01	DNa05	C
3007658	SS00737	GMR_10A12_XA_21-x-GMR_81E05_XD_01	DNp20, DNp22	C
3007659	SS00738	GMR_81D05_XA_21-x-GMR_81E05_XD_01	DNp03, DNp18, DNp20, DNp22	C
3015809	SS01048	BJD_108B07_BB_21-x-BJD_102G01_AV_01	DNd01	C
3015819	SS01058	GMR_21C05_XA_21-x-GMR_28E01_XD_01	DNg09	A
3015826	SS01065	GMR_30C01_BB_21-x-GMR_85H01_XD_01	DNp04	C
3015828	SS01067	GMR_31B08_XA_21-x-GMR_88C07_XD_01	DNp03	D
3015829	SS01068	GMR_32C05_XA_21-x-GMR_70C05_XD_01	DNd02, DNd03	D
3015831	SS01070	GMR_38H06_XA_21-x-GMR_65D06_AV_01	DNa10	C
3015832	SS01071	GMR_40H12_XA_21-x-GMR_85H01_XD_01	DNp04, DNp20	C
3015833	SS01072	GMR_42B02_XA_21-x-GMR_65C02_XD_01	DNg07	B
3015837	SS01076	GMR_50D07_XA_21-x-GMR_74C01_XD_01	DNp04?	C
3016847	SS01548	BJD_112C12_BB_21-x-BJD_104A01_AV_01	DNd02, DNd03	D
3016850	SS01551	BJD_114G06_BB_21-x-BJD_118A10_AV_01	DNg01	C
3016854	SS01555	GMR_10A07_XA_21-x-BJD_104F07_AV_01	DNp27	C
3016867	SS01568	GMR_91C05_XA_21-x-GMR_10A12_XD_01	DNp20	C
3016873	SS01574	BJD_108F02_BB_21-x-BJD_114C04_AV_01	DNg28	B
3016882	SS01583	BJD_119F04_BB_21-x-BJD_100H11_AV_01	DNp11, DNp28	C
3016883	SS01584	BJD_123F06_BB_21-x-GMR_32B03_XD_01	DNg15	C
3016884	SS01585	GMR_10A07_XA_21-x-GMR_24D07_XD_01	DNp27	C
3016891	SS01592	GMR_26E02_XA_21-x-GMR_81D05_XD_01	DNp18, DNp22	C
3016893	SS01594	GMR_29F12_XA_21-x-GMR_24A03_XD_01	DNp02, DNp03, DNp28	C
3016894	SS01595	GMR_29F12_XA_21-x-GMR_31B08_XD_01	DNp03	C
3016897	SS01598	GMR_42B02_XA_21-x-BJD_106H06_AV_01	DNg06	C
3016898	SS01599	GMR_47D05_XA_21-x-GMR_39H12_XD_01	DNa04	C
3016900	SS01601	GMR_59B10_XA_21-x-GMR_21H11_XD_01	DNb02	C
3016902	SS01603	GMR_72H09_XA_21-x-BJD_118A10_AV_01	DNg01	C
3016904	SS01605	GMR_77H03_XA_21-x-GMR_74B04_XD_01	DNb01	C
3018126	SS02260	BJD_106H06_BB_21-x-BJD_112B02_AV_01	DNg06	C
3018533	SS02541	BJD_123E03_BB_21-x-BJD_121E05_AV_01	DNg01	D
3018537	SS02545	GMR_22C05_BB_21-x-BJD_126F02_AV_01	DNa02	C
3018547	SS02555	GMR_81C11_BB_21-x-BJD_126F01_AV_01	DNg11	C
3018644	SS02610	BJD_113F07_BB_21-x-BJD_116F09_AV_01	DNp13	B
3018655	SS02621	GMR_58E07_BB_21-x-GMR_30C01_AV_01	DNp31	C
3020784	SS04160	GMR_38H06_XA_21-x-GMR_50B07_XD_01	DNg14	B
3021403	SS04528	GMR_19G08_BB_21-x-GMR_47F01_XD_01	DNg06	C
3021405	SS04530	GMR_40F04_BB_21-x-GMR_83B06_AV_01	DNc01, DNc02	B
3023061	SS05089	BJD_118C08_BB_21-x-GMR_65C10_AV_01	DNg02	B
3022546	SS05099	GMR_44A07_BB_21-x-BJD_128H06_AV_01	DNg28	B
3023052	SS05107	BJD_110C03_BB_21-x- BJD_118C08_AV_01	DNg02	B
3023055	SS05116	BJD_118C08_BB_21-x- BJD_110C03_AV_01	DNg02	B
3023059	SS05122	BJD_118C08_BB_21-x- BJD_123E03_AV_01	DNg031	B
3023059	SS05122	BJD_118C08_BB_21-x-BJD_123E03_AV_01	DNg01	A

Supplementary Table 5. More broadly expressing DN split-GAL4 lines made in this study.

These lines were not used in the present analysis.

Category	Abbreviation	Full nema
Brain	AL	antennal lobe
	ACA	accessory calyx
	ALA	accessory medulla
	AMMC	antenna-mechanosensory motor center
	AOTU	anterior optic tubercle
	AVLP	anterior ventral protocerebrum
	ATL	antler
	BU	bulb
	CA	calyx
	CAN	cantle
	CNG	cerebral ganglia
	CX	central complex
	CRE	crepine
	EB	ellipsoid body
	EPA	epaullete
	FB	fan-shaped body
	FLA	flange
	GNG	gnathal ganglia
	GOR	gorget
	IB	inferior bridge
	ICL	inferior clamp
	IPS	inferior posterior slope
	LC	lobula columnar cell
	LAL	lateral accessory lobe
	LH	lateral horn
	LO	lobula
	LOP	lobula plate
	LPLC	lobula plate columnar cell
	MB	mushroom body
	ML	medial lobe
	ME	medulla
	NO	noduli
	PED	pedunculus
	PLP	posterior lateral protocerebrum
	PVLP	posterior ventral protocerebrum
	PB	protocerebral bridge
	PRW	proaw
	SAD	saddle
	SCL	superior clamp
	SIP	superior inferior protocerebrum
	SLP	superior lateral protocerebrum
	SMP	superior medial protocerebrum
	SPS	superior posterior slope
VL	vertical lobe	
VES	vest	
WED	wedge	
VNC	AMN	accessory mesothoracic neuromere
	AS	abdominal segment
	DLT	dorsal lateral tract of dorsal cervical fasciculus
	DLV	dorsal lateral tract of ventral cervical fasciculus
	HN	halter neuropil
	ITD	intermediate tract of dorsal cervical fasciculus
	MDA	median dorsal abdominal tract
	MN	mesothoracic neuromere
	MTD	median tract of dorsal cervical fasciculus
	MtN	metathoracic neuromere
	mVAC	medial ventral association center
	NN	neck motor neuropil
	PN	prothoracic neuromere
	VAC	ventral association center
	VLT	ventral lateral tract
	VNC	ventral nerve cord
	VTV	ventral median tract of ventral cervical fasciculus
WN	wing neuropil	

Supplementary Table 6. Abbreviations used.

Additional References for Supplementary Table 2

- Alekseyenko OV, Lee C, Kravitz EA (2010) Targeted manipulation of serotonergic neurotransmission affects the escalation of aggression in adult male *Drosophila melanogaster*. PLoS One 5:e10806.
- Busch S, Selcho M, Ito K, Tanimoto H (2009) A map of octopaminergic neurons in the *Drosophila* brain. J Comp Neurol 513:643-667.
- Gronenberg W, Strausfeld NJ (1992) Premotor descending neurons responding selectively to local visual stimuli in flies. J Comp Neurol 316:87-103.
- Hampel S, Franconville R, Simpson JH, Seeds AM (2015) A neural command circuit for grooming movement control. Elife 4:e08758.
- Ito M, Masuda N, Shinomiya K, Endo K, Ito K (2013) Systematic analysis of neural projections reveals clonal composition of the *Drosophila* brain. Curr Biol 23:644-655.
- Jai YY, Kanai MI, Demir E, Jefferis GS, Dickson BJ (2010) Cellular organization of the neural circuit that drives *Drosophila* courtship behavior. Curr Biol 20:1602-1614.
- Jiang H, Lkhagva A, Daubnerová I, Chae HS, Šimo L, Jung SH, Yoon YK, Lee NR, Seong JY, Žitňan D, Park Y, Kim YJ (2013) Natalisin, a tachykinin-like signaling system, regulates sexual activity and fecundity in insects. Proc Natl Acad Sci USA 110:E3526-2524.
- Kimura, K. I., Hachiya, T., Koganezawa, M., Tazawa, T., & Yamamoto, D. (2008) Fruitless and doublesex coordinate to generate male-specific neurons that can initiate courtship. Neuron 59:759-769.
- Lee, D., Orchard, I., & Lange, A. B. (2013) Evidence for a conserved CCAP-signaling pathway controlling ecdysis in a hemimetabolous insect, *Rhodnius prolixus*. Front Neurosci, 7:207.
- Matsuo, E., Seki, H., Asai, T., Morimoto, T., Miyakawa, H., Ito, K., & Kamikouchi, A. (2016) Organization of projection neurons and local neurons of the primary auditory center in the fruit fly *Drosophila melanogaster*. J Comp Neurol 524:1099-1164.
- Melcher C, Pankratz MJ (2005) Candidate gustatory interneurons modulating feeding behavior in the *Drosophila* brain. PLoS Biol 3:e305.
- Milde JJ, Strausfeld NJ (1990) Cluster organization and response characteristics of the giant fiber pathway of the blowfly *Calliphora erythrocephala*. J Comp Neurol 294:59-75.

- Mu L, Bacon JP, Ito K, Strausfeld NJ (2014) Responses of *Drosophila* giant descending neurons to visual and mechanical stimuli. *J Exp Biol* 217:2121-2129.
- Nässel DR (1993) Neuropeptides in the insect brain: a review. *Cell Tissue Res* 273:1-29.
- Nässel DR, Högmo O, Hallberg E (1984) Antennal receptors in the blowfly *Calliphora erythrocephala*. I. The gigantic central projection of the pedicellar campaniform sensillum. *J Morphol* 180:159-169.
- Nässel DR, Strausfeld NJ (1982) A pair of descending neurons with dendrites in the optic lobes projecting directly to thoracic ganglia of dipterous insects. *Cell Tissue Res* 226:355-362.
- Stocker RF, Lienhard MC, Borst A, Fischbach KF (1990) Neuronal architecture of the antennal lobe in *Drosophila melanogaster*. *Cell Tissue Res* 262:9-34.
- Strausfeld NJ, Bassemir UK (1985) Lobula plate and ocellar interneurons converge onto a cluster of descending neurons leading to neck and leg motor neuropil in *Calliphora erythrocephala*. *Cell Tissue Res* 240:617-640.
- Suver MP, Huda A, Iwasaki N, Safarik S, Dickinson MH (2016) An array of descending visual interneurons encoding self-motion in *Drosophila*. *J Neurosci* 36:11768-11780.
- Tanaka NK, Endo K, Ito K (2012) Organization of antennal lobe-associated neurons in adult *Drosophila melanogaster* brain. *J Comp Neurol* 520:4067-4130.
- Vaughan AG, Zhou C, Manoli DS, Baker BS (2014) Neural pathways for the detection and discrimination of conspecific song in *D. melanogaster*. *Curr Biol* 24:1039-1049.